

A stochastic SIR model for cyber contagion: application to granular growth of firms and to insurance portfolio

Caroline Hillairet^a, Olivier Lopez^a, Lionel Sogouj^{a,b}

^a*CREST, UMR CNRS 9194, Ensaie Paris, Avenue Henry Le Chatelier, 91120 Palaiseau, France*

^b*Institut Louis Bachelier*

Abstract

This work evaluates the impact of contagious cyber-events, over a finite horizon, on firms' financial health and on a cyber insurance portfolio. Our approach builds on key empirical findings from economics and cybersecurity. In economics, firm size and growth-rate distributions are non-Gaussian and exhibit heavy tails. In cybersecurity, contagion dynamics strongly depend on firm size and environmental conditions. To capture these features, we propose a stochastic multi-group SIR model coupled with a granular model of firm growth. This framework allows us to quantify the financial impact of cyber-attacks on firms' revenues and on the insurer's portfolio. In the model, the arrival time and duration of cyber-attacks are driven by a combination of a Cox process and a Bernoulli random variable. The Cox process represents external contagion, with an intensity given by the force of infection derived from the stochastic SIR dynamics. The Bernoulli component captures contagion originating from an infected sister or subsidiary firm. Environmental variability enables stochastic scenario generation and the computation of aggregate exceedance probabilities, a standard metric in catastrophe modeling that provides insurers with immediate insight into the financial severity of an event. We apply the framework to the LockBit ransomware attacks observed between May and July 2024. For a portfolio of 2,929 firms located in Île-de-France, the model predicts that, with 50% probability, the insurer will need to compensate losses equivalent to up to two days of revenue over a 100-day cyber incident.

Keywords: Cyber risk, granular model of firm growth, Aggregate exceedance probability, stochastic stress scenarios, stochastic SIR model, Cox process.

This research is part of the CyFi (Cyber Financialization) project, in cooperation with the cyber risk quantification tech startup *Citalid* and with the financial support of *Bpifrance*.

Introduction

Cybersecurity risk, alongside climate change and geopolitical instability, ranks among the most pressing emerging concerns for experts and the general population (see AXA Group (2025)). It encompasses malicious or accidental events that compromise the confidentiality, availability, or integrity of data and IT services. Common examples include malware infections, service-provider outages, and data breaches. Among these threats, ransomware – a category of malware that prevents or restricts users from accessing their system or exfiltrates sensitive data – with lower barriers to entry, has become one of the most significant threats. GuidePoint Security (2025) reports explosive growth in ransomware attacks: 76.8% between 2022 and 2023, 8.72% between 2023 and 2024, and 58% between 2024 and 2025 in ransomware attacks. In 2025, this amounts to 7,515 publicly reported attacks attributed to up to

124 tracked ransomware groups. Victim organizations face substantial costs, including extortion payments –with AXA Group (2025) reporting \$1.1 billion paid to hackers in 2023–, remediation expenses, legal fees, business interruption losses, and reputational damage. That could consequently represent an increasing part in cyber insurance claims. As a result, there is a growing – not only for businesses but also for financial institutions such as insurance companies, and even for governments – to assess the economic and financial impact of potential future attacks. In this work, we focus on evaluating the impact of a cyber-episode on firms’ financial health and on a cyber insurance portfolio.

Cyber risk modeling in finance and insurance, although relatively recent, encompasses a wide range of approaches. Early contributions rely on traditional frequency–severity frameworks Eling and Loperfido (2017); Farkas et al. (2021), while Edwards et al. (2016) analyze trends in data breaches using Bayesian generalized linear models. More recently, Hawkes processes have been introduced to capture self-excitation and dependence in cyber events. In particular, Bessy-Roland et al. (2021) and Boumezoued et al. (2025) propose multivariate Hawkes models to account for interdependencies between data breaches and the role of vulnerabilities in predicting attack frequency. Beyond point-process approaches, cyber-attacks share key mechanisms with biological epidemics, including the presence of a susceptible population, infection and recovery dynamics, peak intensity, prevalence, and network or cluster structures. This observation has motivated a growing literature inspired by compartmental epidemiological models. In this vein, Hillairet and Lopez (2021) adapt an epidemiological framework to model a contagious cyber event, such as a WannaCry-type attack, and apply it to an insurance portfolio to assess the impact of reaction and remediation measures. This approach is extended in Hillairet et al. (2022) to incorporate the network structure of the firm population. The present work builds on these contributions by designing a cyber episode based on the SIR model, a widely used epidemiological framework, as in Doenges et al. (2024); Ji et al. (2011); Bouzalmat et al. (2023). In its simplest form, the SIR model partitions the population into three compartments:

- susceptible (S) firms that are exposed but not yet infected,
- infected (I) firms that are affected and can transmit the malware,
- and removed (R) firms that have recovered or been secured.

The dynamics of the epidemic are governed by a system of ordinary differential equations describing the transitions between these compartments.

As the application of epidemiological models to cyber insurance remains at an early stage, several important features have yet to be fully incorporated. In this work, we focus on integrating key empirical stylized facts from both economics and cybersecurity. First, firm size and firm structure exhibit pronounced heterogeneity. In particular, Axtell (2001) shows that firm size distributions are heavy-tailed, often following Zipf’s law, while Stanley et al. (1996) documents that firm growth-rate distributions are non-Gaussian. Second, empirical evidence in cybersecurity indicates that the dynamics of cyber-episodes depend strongly on firm size: larger firms are more frequently targeted by cyber-attacks, see Baksy et al. (2025); Kamiya et al. (2021). Moreover, contagion parameters are subject to environmental variability as pointed out by European Central Bank (2025). For instance, in firms organized into multiple subunits, infection rates may differ substantially depending on whether contamination originates

from within the organization or from external sources. Accounting for these sources of heterogeneity is essential for realistically modeling cyber contagion and its financial consequences.

To account for these features, we propose a framework coupling a stochastic multigroup SIR model with a granular growth model for firm revenue. Following the epidemiological approach of Doenges et al. (2024), we study the influence of firm size and distribution on attack propagation. However, rather than the standard conversion of deterministic ODEs into Stochastic Differential Equations (SDEs), we adopt a more intuitive approach by embedding stochasticity directly into the parameters via Cox-Ingersoll-Ross (CIR) processes, as in Allen (2016). To model revenue, we adapt the granular growth framework of Moran et al. (2024), which treats each firm as a collection of subunits with varying degrees of independence. By extending this model into continuous time, we can capture the instantaneous revenue loss occurring at the subunit level during an active attack. The arrival of these attacks is governed by a hybrid process:

- External Contagion: a Cox process with an intensity – the "force of infection"– derived from the SIR model dynamics.
- Internal Contagion: a Bernoulli random variable representing secondary infection from a sister subsidiary.

This mixed process defines both the initial arrival time and the duration of the contagion within a subunit. Finally, we define the insurer's instantaneous cost as the revenue differential between the "no-attack" and "attack" scenarios. At the portfolio level, we quantify risk using the Aggregate Exceedance Probability (AEP) to determine the probability that total losses exceed a defined threshold over a specific horizon. Throughout the paper, we consider a cyber-episode over a finite horizon.

The remainder of this paper is organized as follows. In Section 1, we introduce the jump-diffusion model used to determine the financial health of firms subject to cyber-attacks; we also define the Aggregate Exceedance Probability (AEP) as our primary risk measure for the insurance portfolio. Section 2 is dedicated to the cyber-attack contagion model, providing analytical results that establish the existence and uniqueness of a non-negative solution for the stochastic multi-group SIR framework. In Section 3, we bridge these frameworks by translating the contagious cyber-episode into the jump-diffusion revenue model using internal and external transmission probabilities. Finally, Section 4 details our data sources, model calibration, and simulation results. Specifically, the contagion model is validated using data from the ransomware episode attributed to the Lockbit group (May - July 2024), and its impact is assessed on a representative portfolio of 2,929 firms in the Île-de-France region.

1. Firm value and insurance portfolio dynamics under cyber-attacks

In this section, we extend the granular model of firm growth of Wyart and Bouchaud (2003); Herskovic et al. (2020); Moran et al. (2024) in a continuous time setting and in the context of cyber risk. This model has been introduced to fit some empirical facts, in particular the ones cited by Stanley et al. (1996); AXA Group (2025): both the firm size distribution and the growth rate distribution are non-Gaussian and feature heavy tails.

Throughout this work we consider a probability space $(\Omega, \mathcal{A}, \mathbb{P})$, where \mathcal{A} is a σ -algebra on Ω . We fix $T > 0$ which represents the horizon of the cyber-episode. In the same spirit as Moran et al. (2024), within a given insurance portfolio of $H \in \mathbb{N}^*$ firms characterized by exogenous production, we consider that firms are composed of a number of independent subunits, such as departments or production units, which operate within separate sub-markets and which are not necessarily of equal size. We have the following assumption.

Assumption 1.1. The revenue of firm $i \in \{1, \dots, H\}$ at time $t \geq 0$ is denoted by $Z_{i,t}$ and satisfies

$$Z_{i,t} := \sum_{j=1}^{K_i} z_{ij,t}, \quad (1.1)$$

where $K_i \in \mathbb{N}^*$ represents the number of subunits and $z_{ij,t}$, $j = 1, \dots, K_i$, denotes the respective revenue.

We will note

$$\mathcal{I} := \{(i, j) \mid i \in \{1, \dots, H\} \text{ and } j \in \{1, \dots, K_i\}\}. \quad (1.2)$$

The firm's size is the number of its subunits, and the revenue is an indicator of firms' and subunits' financial health. Instead of revenue, we could consider its workforce, profits, etc. In addition, we could view the economy as a supra-firm subdivided in sectors. In the same way, each sector can be seen as a supra-firm subdivided in companies. This point of view could be interesting for calibration because public data are usually more easily available at economy/sectoral level than at firm's level. The firm's size K_i , which is an integer, is a random variable assumed to be distributed according to Zipf's law (the discrete version of Pareto distribution) on $\{1, \dots, K\}$, $K \in \mathbb{N}^*$. For $k = 1, \dots, K$

$$\mathbb{P}(K_i = k) = q \frac{\mathbf{a}k^{-(1+\mathbf{a})}}{1 - K^{-\mathbf{a}}}; \quad 1 < \mathbf{a} < 2. \quad (1.3)$$

The above assumption is motivated by the literature (see Wyart and Bouchaud (2003); Moran et al. (2024)) and is easily verified on the data (see Figure 4a and Figure 4b where $\mathbf{a} = 1.76$ and $q = 0.784$).

1.1. The impact of cyber-attacks on firms' revenue

When a cyber-attack succeeds, it causes financial loss to the company. This loss can result from paying a ransom, business disruption, repairing equipment, reputation costs, etc. Let $1 \leq i \leq H$ and $1 \leq j \leq K_i$. In the absence of a cyber-attack, the revenue z_{ij} of subunit j of firm i is modeled as a Geometric Brownian motion, while in the presence of a cyber-attack, it is modeled as a jump-diffusive process. We introduce the following assumption.

Assumption 1.2. For $(i, j) \in \mathcal{I}$,

1. Without the cyber-event, the time evolution of each subunit i 's revenue, \bar{z}_{ij} , is characterized by the diffusion process

$$\frac{d\bar{z}_{ij,t}}{\bar{z}_{ij,t}} = \mu_{ij}dt + \sigma_{ij}dB_{ij,t}, \quad \bar{z}_{ij,0} = z_{ij,0} > 0, \sigma_{ij} > 0, \mu_{ij} \in \mathbb{R}, \quad (1.4)$$

where B_{ij} is a Brownian motion. For a given firm i , $1 \leq i \leq H$, the Brownian motions $(B_{ij})_{1 \leq j \leq K_i}$ driving the revenues of the subunits are correlated with correlation coefficient $\rho_i \in \mathbb{R}$. But for different firms $i_1 \neq i_2$, $B_{i_1 j_1}$ and $B_{i_2 j_2}$ are assumed to be independent. Integrating SDE (1.4), we have

$$\bar{z}_{ij,t} = z_{ij,0} \exp \left(\left(\mu_{ij} - \frac{\sigma_{ij}^2}{2} \right) t + \sigma_{ij} B_{ij,t} \right).$$

2. The random time τ_{ij} of the arrival of the cyber-attack affecting the subunit j of firm i , is defined as

$$\tau_{ij} = \inf\{t \geq 0 | N_{ij,t} \geq 1\}, \quad (1.5)$$

where $N_{ij,t}$ is a point process that will be defined later.

3. δ_{ij} is a random time representing the duration of an infection.
4. We introduce the process π_{ij} , taking values in $[0, 1]$, which represents the random fraction of the firm's revenue lost during the infection.

Therefore, the firm's revenue $z_{ij,t}$ evolves as follows

$$z_{ij,t} = \begin{cases} \bar{z}_{ij,t} & \text{if } t < \tau_{ij} \\ (1 - \pi_{ij,t}) \bar{z}_{ij,t} & \text{if } \tau_{ij} \leq t < \tau_{ij} + \delta_{ij} \\ \bar{z}_{ij,t} & \text{if } t \geq \tau_{ij} + \delta_{ij} \end{cases} \quad (1.6)$$

Moreover, $(\pi_{ij})_{(i,j) \in \mathcal{I}}$, $(N_{ij})_{(i,j) \in \mathcal{I}}$, and $(B_{ij})_{(i,j) \in \mathcal{I}}$ are assumed to be independent.

Let $(i, j) \in \mathcal{I}$. In the above assumption, the constant parameters σ_{ij} (resp. μ_{ij}) define the order of magnitude (resp. the drift) of the growth fluctuations at the level of a subunit. Regarding random time τ_{ij} , for $t \geq 0$ and the subunit (i, j) , the event $\{\tau_{ij} \leq t\}$ corresponds to a successful breach caused by an attack on before time t ; otherwise, no attack has taken place yet or the potential attack is blocked and no loss occurs before time t . It should also be noted that the K_i -dimensional process $(N_{ij})_{1 \leq j \leq K_i}$ is potentially correlated, because there can be internal contamination between subsidiaries, as we will see later. Moreover, the property on the Brownian motion $(B_{ij})_{ij}$ means that inside the same firm, the subunits' revenues are correlated but different firms' revenues are not.

Finally, the process π_{ij} represents the severity (i.e. the instantaneous random monetary loss) of the attack. This loss may be potentially covered by an insurance contract. It is a $[0, 1]$ -value process because a cyber-attack is detrimental to the subunit, but its losses remain capped at its potential earnings. The time-behavior of the loss process may depend on the dynamics of the epidemic, on the firm's investments in cybersecurity, and also on cyber insurance premium: the severity might begin high when infection starts, and progressively drop to zero (full recovery). Or, it could start slowly, peak, and then decline. Having no explicit empirical input on this feature, we limit ourselves in this work to the case where the severity does not depend on time, so π_{ij} is a random variable instead of a stochastic process. The sequence $(\pi_{ij})_{ij}$ are assumed independent and identically distributed with common distribution f_π having support in $[0, 1]$, mean π_\star and standard deviation σ_\star^2 .

Example 1.3 (Beta distribution). For the numerical analysis, we will take $\pi_{ij} \sim B(\alpha^\pi, \beta^\pi)$ whose density probability function is $f(x; \alpha^\pi, \beta^\pi) = \frac{x^{\alpha^\pi-1}(1-x)^{\beta^\pi-1}}{B(\alpha^\pi, \beta^\pi)}$ for $x \in [0, 1]$ where $B(\alpha^\pi, \beta^\pi) = \frac{\Gamma(\alpha^\pi)\Gamma(\beta^\pi)}{\Gamma(\alpha^\pi+\beta^\pi)}$ and Γ is the Gamma function.

If we are dealing with the whole portfolio (or a whole sector or an entire economy), we can also derive the total output (revenue) \mathbf{O} so that for all $t \geq 0$,

$$\mathbf{O}_t := \sum_{i=1}^H Z_{i,t}, \quad (1.7)$$

where the individual firm revenue is given by

$$Z_{i,t} = \sum_{j=1}^{K_i} (1 - \pi_{ij} \mathbf{1}_{\tau_{ij} \leq t < \tau_{ij} + \delta_{ij}}) \bar{z}_{ij,t} = \sum_{j=1}^{K_i} (1 - \pi_{ij} \mathbf{1}_{\tau_{ij} \leq t < \tau_{ij} + \delta_{ij}}) z_{ij,0} \exp \left(\left(\mu_{ij} - \frac{\sigma_{ij}^2}{2} \right) t + \sigma_{ij} B_{ij,t} \right).$$

We also introduce the natural filtration of $(B_{ij})_{(i,j) \in \mathcal{I}}$

$$\mathbb{F}^B := (\mathcal{F}_t^B)_{t \geq 0}. \quad (1.8)$$

1.2. The impact of cyber-attack on insurance portfolio

Based on the description of the attack at the policyholder level, the insurance company is interested in aggregating these risks. We focus on the total claims of the cyber-event for the insurance company over a period. For a policyholder experiencing a cyber-attack, each day spent infected results in financial losses: their revenue decreases. The insurance company potentially compensates a part (or all) of these losses. Consider the policyholder $i \in \{1, \dots, H\}$. For all $j \in \{1, \dots, K_i\}$, recall the dynamics of the subunit's revenue without and with the cyber risk \bar{z}_{ij} and z_{ij} respectively in (1.4) and in (1.6). We then define the instantaneous claim for policyholder i :

Definition 1.4. For $1 \leq i \leq H$, the process \mathbf{c}_i , corresponding to the instantaneous claim for policyholder i at time $t \geq 0$, is defined as

$$\mathbf{c}_{i,t} := - \sum_{j=1}^{K_i} (z_{ij,t} - \bar{z}_{ij,t}) = \sum_{j=1}^{K_i} \pi_{ij} \mathbf{1}_{\tau_{ij} \leq t < \tau_{ij} + \delta_{ij}} z_{ij,0} \exp \left(\left(\mu_{ij} - \frac{\sigma_{ij}^2}{2} \right) t + \sigma_{ij} B_{ij,t} \right). \quad (1.9)$$

This represents the sum of the differences in income for each sub-unit, with and without a cyber-attack.

A key metric for the insurer for quantifying the impact of attacks is the Cumulative Distribution Function (CDF) of the portfolio's total losses, with an emphasis on extreme losses that could threaten liquidity. We focus first on losses over short intervals, such as a single day.

Definition 1.5. For $t, u \geq 0$, the cumulative distribution function of the portfolio over the period $[t, t+u]$ is denoted, for all $x \geq 0$,

$$\mathbf{F}_{[t,t+u]}(x) := \mathbb{P} \left(\sum_{i=1}^H C_{i,[t,t+u]} \leq x \right), \quad (1.10)$$

where for $1 \leq i \leq H$, $C_{i,[t,t+u]}$ is the total claim of firm i between t and $t + u$

$$C_{i,[t,t+u]} := \int_t^{t+u} c_{i,s} ds = \sum_{j=1}^{K_i} z_{ij,0} \int_{t \vee \tau_{ij}}^{(t+u) \wedge (\tau_{ij} + \delta_{ij})} \pi_{ij} e^{\left(\mu_{ij} - \frac{\sigma_{ij}^2}{2}\right)s + \sigma_{ij} B_{ij,s}} ds. \quad (1.11)$$

In order to measure the overall severity of the attack, we next introduce a widely used metric in catastrophe risk modeling: the Aggregate Exceedance Probability or AEP (see Grossi et al. (2005); Homer and Li (2017)). It is the probability that the sum of several cyber-incidents losses over a period exceeds a certain amount. In general, AEP is computed on one year, but we define here AEP on the horizon of the epidemic T . For a given cyber-episode lasting until date T , the total portfolio loss due to this episode over $[0, T]$, is denoted \mathfrak{C}_T

$$\mathfrak{C}_T := \sum_{i=1}^H \left(\int_0^T c_{i,t} dt \right) = \sum_{i=1}^H C_{i,[0,T]}. \quad (1.12)$$

The AEP calculates the impact of several identical cyber-incidents that occurred during the period $[0, T]$.

Definition 1.6. Over the period $[0, T]$, the insurance portfolio can be affected by a random number P of cyber-events, each of them leading to a random claim amount \mathfrak{C}_T^p , $p = 1, \dots, P$. We assume the random claim amounts $(\mathfrak{C}_T^p)_p$ to be independent and identically distributed according to $\mathbf{F}_{[0,T]}$ (that is the distribution of \mathfrak{C}_T defined in (1.12)), and independent of P . Then the Aggregate Exceedance Probability (AEP) at time T is defined as, for $x \geq 0$,

$$\text{AEP}_T(x) := \mathbb{P}(\mathfrak{C}_T^1 + \mathfrak{C}_T^2 + \dots + \mathfrak{C}_T^P > x). \quad (1.13)$$

Computing AEP_T requires the convolution of the CDF of \mathfrak{C}_T , $\mathbf{F}_{[0,T]}$ defined in (1.10). For $p \in \mathbb{N}$, let $\mathbf{F}_{\mathfrak{C}_T}^{(p)}$ denote the p -fold convolution of $\mathbf{F}_{[0,T]}$ defined iteratively as

$$\mathbf{F}_{\mathfrak{C}_T}^{(1)} = \mathbf{F}_{[0,T]}, \quad \mathbf{F}_{\mathfrak{C}_T}^{(p)}(x) = \int_0^x \mathbf{F}_{\mathfrak{C}_T}^{(p-1)}(x-y) \mathbf{f}_{[0,T]}(y) dy, \quad p = 2, 3, \dots,$$

with $\mathbf{f}_{[0,T]}$ the probability density function associated with $\mathbf{F}_{[0,T]}$. Then, given that P is independent of the claim amounts (\mathfrak{C}_T^p) , we have by the law of total probability, for¹ $x > 0$

$$\begin{aligned} \text{AEP}_T(x) &= \sum_{p=1}^{+\infty} \mathbb{P}(\mathfrak{C}_T^1 + \mathfrak{C}_T^2 + \dots + \mathfrak{C}_T^p > x | P = p) \mathbb{P}[P = p] \\ &= 1 - \sum_{p=1}^{+\infty} \mathbf{F}_{\mathfrak{C}_T}^{(p)}(x) \mathbb{P}[P = p] = 1 - \mathbb{E}_P \left[\mathbf{F}_{\mathfrak{C}_T}^{(P)}(x) \right] \\ &= \mathbb{E}_P \left[\mathbb{P} \left(\sum_{k=1}^P \mathfrak{C}_T^k > x \right) \right]. \end{aligned} \quad (1.14)$$

¹Obviously $\text{AEP}_T(0) = 1$.

In the numerical section, the latter quantity is computed via a Monte Carlo simulation.

All the above metrics require to know the distribution of the processes $(c_{i,t})_t$ for each i . The sources of randomness in these quantities are the processes $(B_{ij,t})$, $(N_{ij,t})$, and the variables (π_{ij}) . In order to evaluate the impact of cyber incidents on an economy (using (1.7)) or on an insurance portfolio (using (1.14)), a crucial point is to model the cyber contagion or in other words, the dynamics of the process $(N_{ij})_{ij}$. Early works such as Peng et al. (2017) or Zeller and Scherer (2022) model the arrival of cyber-attacks using (in)homogeneous Poisson processes. Thereafter, Bessy-Roland et al. (2021) and Boumezoued et al. (2025) show that Hawkes processes are particularly suitable to capture the contagion phenomena, the clustering, and the autocorrelation of the arrival times of cyber incidents. Lastly, by noting that a cyber incident and a biological epidemic have similar characteristics, Hillairet and Lopez (2021) and Hillairet et al. (2022) use compartmental epidemiological models to describe cyber contagion by linking the hazard rate function of arrival times with the dynamics of infected individuals. We adapt the latter approach in the present work because our purpose is to model the dynamics of a specific cyber-contagion over a finite time horizon.

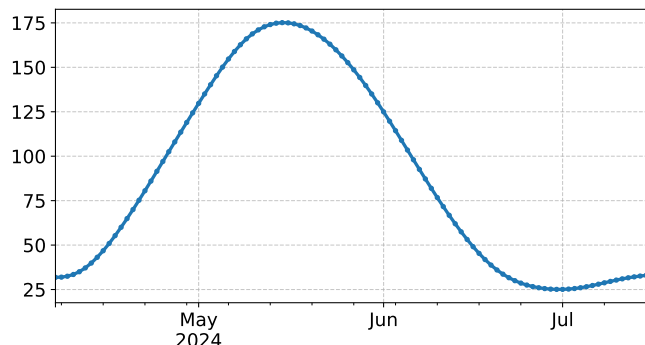
2. The contagion model

As suggested by Figure 1 (from the 2025 Ransomware & Cyber Threat Report of *GuidePoint Security's Research and Intelligence Team's [GRIT]*), biological epidemics and cyber contagion episodes have fairly similar characteristics. Much like certain contagious biological outbreaks, a firm (just as a person) could be susceptible i.e. not yet infected but vulnerable if exposed to an infectious firm, infected i.e. affected by the malware and which can transmit, and removed or recovered i.e. whose systems are cured, secured, or patched. Moreover, when examining the dynamics of companies infected by the LockBit ransomware between May and July 2024 on Figure 1a, the number of infections starts out low, then escalates rapidly until it reaches a peak, before beginning to decline. Finally, just as infection rates differ within and between households in biological epidemics, cyber epidemics mirror this transmission pattern within and between firms' subunits. Subsidiaries of a given company are, by nature, more interconnected together than with external organizations.

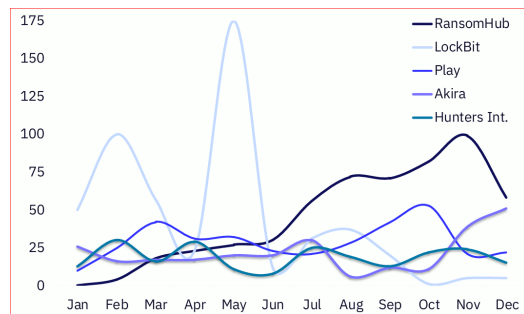
2.1. The model

To model the infection process within a firm, we adapt the SIR for households proposed by Doenges et al. (2024). Precisely, we extend their deterministic SIR into a stochastic SIR in the sense that the model parameters are no longer deterministic but instead follow a Cox–Ingersoll–Ross dynamic. As Hillairet and Lopez (2021), we assume that contagion does not come from inside the portfolio itself, but from outside, so that the spread of the attack is defined as a global level. We view a cyber infectious event in a fully susceptible firm of size $k \in \{1, \dots, K\}$ as a splitting process generating a infected firm of size j , where $1 \leq j \leq k$ and a remaining susceptible firm of size $k - j$. Let s_j , i_j and r_j denote the number of susceptible, infected, and removed firms of size j , where $1 \leq j \leq K$. The quantity K , introduced in Equation (1.3), represents the maximal size of a firm. We denote the processes

- $h_j = s_j + i_j + r_j$ equals to the total number of current firms of size j ;



(a) Number of infected from LockBit reported from May to July 2024 (Date in days on the x-axis and number of companies attacked on the y-axis)



(b) Most Impactful Ransomware in 2024 (the date in months on the x-axis and the number of companies attacked on the y-axis)

Figure 1: GRIT 2025 Ransomware & Cyber Threat Report (see GuidePoint Security (2025))

- $h = \sum_{j=1}^K h_j$ is the total number of firms;
- The total population (number of subunits) is given by $n = \sum_{j=1}^K j h_j$.

Rather than working with the number of susceptible/infected/removed firms which are integers and not fully adapted to the ODE, we introduce for all $1 \leq j \leq K$, $S_j := s_j/h$, $I_j := i_j/h$, $R_j := r_j/h$, and $H_j := h_j/h$ the fraction of susceptible, infected, removed, and all firms of size j respectively. We thus write the average size of firm as

$$N = \sum_{j=1}^K j H_j. \quad (2.1)$$

Let us now describe how the cyber-infection spreads into the subunits. Let j range from 1 to K .

1. If an initial infection is brought into a susceptible firm of size j , secondary infections will occur inside the firm.
2. Each of the remaining $j-1$ firm members can get infected with equal probability a . This represents the "in-firm" infection rate.
3. The probability that a primary infection in a firm of size j generates in total k infections inside this firm is $b_{j,k}$, where $1 \leq k \leq j$.
4. The secondary infections give rise to a splitting of the initial firm of size j into a new, fully infected firm of size k and another still susceptible firm of size $j-k$.
5. An infected firm of size k contributes to the overall force of infection between different firms and recovers with a rate γ_k .
6. β_k is the "out-firm" infection rate which refers to infection events occurring between different firms and hence outside a given single firm.

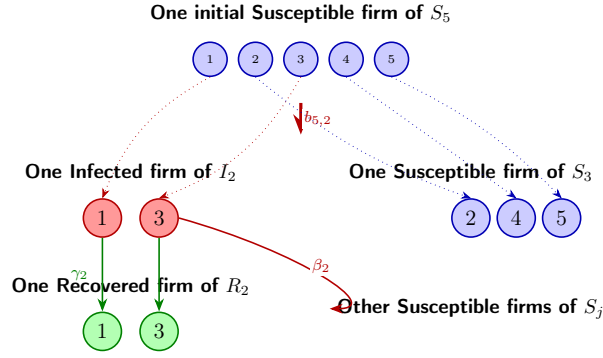


Figure 2: Infection and Splitting: $S_5 \rightarrow I_2 + S_3$

The graph in Figure 2 above gives an example where $k = 5$ and $j = 2$. We summarize and precise these features in the following assumption.

Assumption 2.1. The dynamic system governing the dynamics of the susceptible, infected and removed firms of size k reads as

$$\begin{cases} \frac{dS_{k,t}}{dt} = Y_t \left(-kS_{k,t} + \sum_{j=k+1}^K jS_{j,t} \cdot b_{jj-k,t} \right), & (2.2) \\ \frac{dI_{k,t}}{dt} = -\gamma_{k,t}I_{k,t} + Y_t \sum_{j=k}^K jS_{j,t} \cdot b_{jk,t}, & (2.3) \\ \frac{dR_{k,t}}{dt} = \gamma_{k,t}I_{k,t}, & (2.4) \end{cases}$$

where

$$Y_t = \frac{1}{N_t} \sum_{k=1}^K \beta_{k,t} \cdot kI_{k,t} \quad (2.5)$$

is the total force of infection – the instantaneous risk that a susceptible individual becomes infected. Let us note the set of $(2K + K^2)$ stochastic parameters

$$\Psi := \{\beta_1, \dots, \beta_K, \gamma_1, \dots, \gamma_K, b_{11}, \dots, b_{1K}, b_{21}, \dots, b_{K-1K}, b_{KK}\}.$$

We assume that a parameter $\varphi \in \{b_{11}, \dots, b_{1K}, b_{21}, \dots, b_{K-1K}, b_{KK}\}$ is a $[0, 1]$ -valued process $\varphi = \frac{1}{1+e^{-\tilde{\varphi}}}$ where $\tilde{\varphi}$ evolves according to the Cox-Ingersoll-Ross (CIR) dynamics

$$d\tilde{\varphi}_t = \kappa_\varphi(\mu_\varphi - \tilde{\varphi}_t)dt + \Sigma_\varphi \sqrt{\tilde{\varphi}_t} d\mathcal{W}_{\varphi,t}, \quad \mu_\varphi \in \mathbb{R}, \Sigma_\varphi > 0, \kappa_\varphi > 0, \varphi_0 \geq 0, \quad (2.6)$$

while $\varphi \in \{\beta_1, \dots, \beta_K, \gamma_1, \dots, \gamma_K\}$ is also assumed to be a CIR process.

In both case, the parameters satisfy Feller conditions i.e. $2\kappa_\varphi\mu_\varphi \geq \Sigma_\varphi^2$. Moreover, $(\mathcal{W}_\varphi)_{\varphi \in \Psi}$ is a $(2K + K^2)$ -dimensional Brownian motion, independent to $(B_{ij})_{(i,j) \in \mathcal{I}}$ (defined in Assumption 1.2).

Recall that the expectation and variance of a CIR process (2.6) is given by (see Cox et al. (1985)): for $t \geq 0$,

$$\mathbb{E}[\tilde{\varphi}_t] = \varphi_0 e^{-\kappa_\varphi t} + \mu_\varphi (1 - e^{-\kappa_\varphi t}), \quad \mathbb{V}[\tilde{\varphi}_t] = \varphi_0 \frac{\Sigma_\varphi^2}{\kappa_\varphi} (e^{-\kappa_\varphi t} - e^{-2\kappa_\varphi t}) + \frac{\mu_\varphi \Sigma_\varphi^2}{2\kappa_\varphi} (1 - e^{-\kappa_\varphi t})^2.$$

Remark 2.2. In this SIR model, the average size process defined in (2.1)

$$N = \sum_{k=1}^K k(S_k + I_k + R_k),$$

does not depend on t . From now on, we will write N_0 instead of N_t to refer to the average size.

We could have used a SIRS model that allows an infected-and-removed unit to become susceptible again and be reinfected, but we can ignore this feature since we are dealing with a short-lived cyber incident. In other words, there is not enough time for a unit to be infected multiple times.

The details on the deterministic version of this model are detailed in Doenges et al. (2024). The stochasticity in the epidemiological model is motivated by the fact that fluctuations in the environment affect models' parameters. Several works in the literature introduce randomness by simply transforming the model from a system of ODEs to a system of SDEs. This implies that the randomness comes from a single parameter (for example on transmission coefficient between compartments for Ji et al. (2011) or on the the decay rate of immunity for Bouzalmat et al. (2023)). However, since all the parameters can be subject to environmental variability, it appears more natural to consider each parameter having its own stochastic dynamics.

We define the (right continuous and complete) filtration $\mathbb{F}^{\mathcal{W}} = (\mathcal{F}_t^{\mathcal{W}})_{t \geq 0}$ generated by the stochastic parameters: for $t \geq 0$,

$$\mathcal{F}_t^{\mathcal{W}} := \sigma(\{\mathcal{W}_{\varphi,s}, s \leq t \text{ and } \varphi \in \Psi\}). \quad (2.7)$$

Remark 2.3. For the numerical analysis, the infections inside the firm is modeled by a Bernoulli-process with in-firm attack rate (infection probability) $a \in [0, 1]$, and the total number of infected subunit inside the firm follows a binomial distribution, namely, for $1 \leq j, k \leq K$,

$$b_{jk} = \binom{j-1}{k-1} a^{k-1} (1-a)^{j-k}. \quad (2.8)$$

Next, we also assume that $a = \frac{1}{1+e^{-\tilde{a}}} \in [0, 1]$ where the process \tilde{a} is governed by a CIR dynamics. This assumption reduces the dimension of the set Ψ from $2K + K^2$ to $2K + 1$ and ease the calibration process.

2.2. Existence and uniqueness of the nonnegative solution of the SIR system

This section is dedicated to the existence and uniqueness result of a nonnegative solution to the system (2.2)-(2.3)-(2.4). The following theorem and its proof are inspired by Ji et al. (2011).

Theorem 2.4 (Existence and uniqueness). *Consider the system (2.2)-(2.3)-(2.4).*

1. For $\omega \in \Omega$, $t_0 \geq 0$, and for any initial value $(S_{t_0}, I_{t_0}, R_{t_0}) \in \mathbb{R}_+^{3 \times K}$, there is an unique global solution $(S_t(\omega), I_t(\omega), R_t(\omega))_{t \geq t_0}$ in $\mathbb{R}_+^{3 \times K}$ of system (2.2)-(2.3)-(2.4).
2. S , I , and R are $\mathbb{F}^{\mathcal{W}}$ -adapted.

Proof. The differential system (2.2)-(2.3)-(2.4) is an ordinary differential equation (ODE) with stochastic coefficients sometimes abusively called stochastic differential equation (SDE).

1. Consider the "associated" deterministic ODE i.e. the one associated with a fixed sample path. For a fixed $\omega \in \Omega$, the system becomes

$$\begin{cases} \frac{dS_{k,t}(\omega)}{dt} = -kY_t(\omega)S_{k,t}(\omega) + Y_t(\omega) \sum_{j=k+1}^K jS_{j,t}(\omega) \cdot b_{jj-k,t}(\omega), & (2.9) \\ \frac{dI_{k,t}(\omega)}{dt} = -\gamma_{k,t}(\omega)I_{k,t}(\omega) + Y_t(\omega) \sum_{j=k}^K jS_{j,t}(\omega) \cdot b_{jk,t}(\omega), & (2.10) \\ \frac{dR_{k,t}(\omega)}{dt} = \gamma_{k,t}(\omega)I_{k,t}(\omega), & (2.11) \end{cases}$$

where

$$Y_t(\omega) = \frac{1}{N_0} \sum_{k=1}^K \beta_{k,t}(\omega) \cdot kI_{k,t}(\omega). \quad (2.12)$$

In the above equation, both the variables S, I, R, Y and the parameters $\beta_1, \dots, \beta_K, \gamma_1, \dots, \gamma_K, b_{11}, \dots, b_{1K}, b_{21}, \dots, b_{KK}$ depend on ω . However, we will not specify it further in order to lighten the notation. The system can be rewritten in the following form

$$(\dot{S}, \dot{I}, \dot{R}) = F(S, I, R, \omega),$$

where $F(S, I, R, \omega)$ corresponds to the right hand side of the system (2.9)-(2.10)-(2.11). The function F is locally Lipschitz continuous, for any given initial value $(S_{t_0}, I_{t_0}, R_{t_0}) \in \mathbb{R}_+^{3 \times K}$: according to Picard-Lindelöf theorem, there is an unique local solution (S_t, I_t, R_t) on $t \geq t_0$, for any $t_0 \geq 0$. From (2.10), we have

$$\frac{dI_{k,t}}{dt} = -\gamma_{k,t}I_{k,t} + Y_t \sum_{j=k}^K jS_{j,t} \cdot b_{jk,t} \geq -\gamma_{k,t}I_{k,t},$$

then $\frac{dI_{k,t}}{I_{k,t}} \geq -\gamma_{k,t}dt$, which implies that

$$I_{k,t} \geq I_{k,t_0} \exp\left(-\int_{t_0}^t \gamma_{k,s} ds\right) \geq 0.$$

From (2.11), by noticing that $\frac{dR_{k,t}}{dt} \geq -\alpha_{k,t}R_{k,t}$, and from (2.9), by noticing that $Y_t \leq 1$ and $\frac{dS_{k,t}}{dt} \geq -kS_{k,t}$, we also conclude that $S_{k,t} \geq 0$ and $R_{k,t} \geq 0$. However, from Remark 2.2, the average size of firm N is constant and equals to N_0 , consequently the local solution can be extended to a global one and belongs to $\mathbb{R}_+^{3 \times K}$.

2. When a solution exists, the second item is straightforward. Since each coefficient $\varphi \in \Psi$ satisfies Lipschitz and linear growth conditions, there exists a unique strong solution, namely,

$$\tilde{\varphi}_t = \varphi_0 e^{-\kappa_\varphi t} + \mu_\varphi (1 - e^{-\kappa_\varphi t}) + \Sigma_\varphi \int_0^t e^{-\kappa_\varphi(t-s)} \sqrt{\tilde{\varphi}_s} d\mathcal{W}_{\varphi,s}, \quad \text{for all } t \geq 0 \quad (2.13)$$

which is $\mathbb{F}^{\mathcal{W}}$ -adapted. Therefore all coefficients φ of the system (2.2)-(2.3)-(2.4) are $\mathbb{F}^{\mathcal{W}}$ -adapted, whose unique solution (S, IR) is also $\mathbb{F}^{\mathcal{W}}$ -adapted.

□

To analyze the spread of the cyber-attack, we can introduce additional quantities such as the prevalence which is a non-negative process representing the fraction of recovered subunits,

$$\mathfrak{P} := \frac{1}{N_0} \sum_{k=1}^K k R_k \quad (2.14)$$

and the peak, a random variable representing the maximum of total number of infected subunits,

$$\mathfrak{J} := \max_{t \geq 0} \sum_{k=1}^K k I_{k,t}. \quad (2.15)$$

Also in epidemiology modeling literature, the basic reproduction number is the number of new infections produced by a typical infective individual in a population at a Disease Free Equilibrium (DFE), the state at which a population remains in the absence of disease. It is used to determine if the disease always dies out (after some time) or if it persists (around an endemic equilibrium). When the model parameters are constant, Doenges et al. (2024) shows that the basic reproduction number R_0 is

$$R_0 = \sum_{i=1}^K i \frac{\beta_i}{\gamma_i} \sum_{m=i}^K \frac{m S_m}{N_0} \cdot b_{m,i}. \quad (2.16)$$

Moreover, some works such as Van den Driessche and Watmough (2002); Guo et al. (2006) show that, if the model admits a DFE, then the latter is locally asymptotically stable if $R_0 < 1$. Similar results exist for the stochastic case but where the randomness is introduced by using a system of SDE instead of a system of ODE (see Ji et al. (2011)). The following theorem provides a basic reproduction number and a local stability condition for the dynamic contagion model developed in this paper.

Theorem 2.5 (Necessary condition for the local stability). *Let $t \geq 0$. If*

$$\mathcal{R}_{max,t} := \left[\max_{1 \leq k \leq K} \frac{\beta_{k,t}}{\gamma_{k,t}} \right] \sum_{i=1}^K i \sum_{m=i}^K \frac{m S_{m,t}}{N_0} \cdot b_{mi,t} < 1, \quad (2.17)$$

then $\frac{d \log \mathfrak{J}_t}{dt} < 0$.

Proof. Let $t \geq 0$, from (2.15), we have

$$\mathfrak{J}'_t = \sum_{k=1}^K k I'_{k,t} = \sum_{k=1}^K k \left(-\gamma_{k,t} I_{k,t} + Y_t \sum_{j=k}^K j S_{j,t} \cdot b_{jk,t} \right).$$

By applying the Itô formula

$$\begin{aligned} \frac{d \log \mathfrak{J}_t}{dt} &= \frac{d\mathfrak{J}_t}{dt} \frac{1}{\mathfrak{J}_t} = -\frac{1}{\mathfrak{J}_t} \sum_{k=1}^K k \gamma_{k,t} I_{k,t} + Y_t \sum_{k=1}^K k \sum_{j=k}^K j S_{j,t} \cdot b_{jk,t} \\ &= -\frac{1}{\mathfrak{J}_t} \left(\sum_{k=1}^K k \gamma_{k,t} I_{k,t} - \frac{1}{N_0} \sum_{k=1}^K \beta_{k,t} \cdot k I_{k,t} \sum_{i=1}^K i \sum_{m=i}^K m S_{m,t} \cdot b_{mi,t} \right) \\ &= -\frac{1}{\mathfrak{J}_t} \sum_{k=1}^K k \gamma_{k,t} I_{k,t} \left(1 - \frac{\beta_{k,t}}{\gamma_{k,t}} \sum_{i=1}^K i \sum_{m=i}^K \frac{m S_{m,t}}{N_0} \cdot b_{mi,t} \right) \\ &= -\sum_{k=1}^K \frac{k \gamma_{k,t} I_{k,t}}{\mathfrak{J}_t} (1 - \mathcal{R}_{k,t}), \end{aligned}$$

where we denote

$$\mathcal{R}_{k,t} := \frac{\beta_{k,t}}{\gamma_{k,t}} \sum_{i=1}^K i \sum_{m=i}^K \frac{m S_{m,t}}{N_0} \cdot b_{mi,t}. \quad (2.18)$$

With \mathcal{R}_{max} defined in (2.17), we have

$$\mathcal{R}_{k,t} \leq \mathcal{R}_{max,t}.$$

Therefore $1 - \mathcal{R}_{max,t} \leq 1 - \mathcal{R}_{k,t}$ and since $\frac{-k \gamma_{k,t} I_{k,t}}{\mathfrak{J}_t} \leq 0$, we have

$$\frac{d \log \mathfrak{J}_t}{dt} \leq -\sum_{k=1}^K \frac{k \gamma_{k,t} I_{k,t}}{\mathfrak{J}_t} (1 - \mathcal{R}_{max,t}),$$

which is negative when $\mathcal{R}_{max,t} < 1$. □

In addition, if $\mathcal{R}_\infty := \max_{t \geq 0} \{\mathcal{R}_{max,t}\} < 1$, we can easily show that there exists $h < 0$ such that

$$\limsup_{T \rightarrow +\infty} \frac{\log \mathfrak{J}_T}{T} \leq h. \quad (2.19)$$

Remark 2.6. We can also make the following remarks:

- In our framework, $\mathcal{R}_{max,t}$ (respectively \mathcal{R}_∞) represents the local (respectively global) basic reproduction number.

- In addition to the model parameters, both $\mathcal{R}_{max,t}$ and \mathcal{R}_∞ can depend on the trajectories of susceptible subunits $(S_{m,t})_{1 \leq m \leq K, t \geq 0}$. When $\frac{\beta_{k,t}}{\gamma_{k,t}}$ is independent of k and t and $b_{mi,t}$ independent of t as in Doenges et al. (2024), we retrieve exactly the expected R_0 given in (2.16).
- It is obvious that $\mathfrak{J} \geq 0$ and Theorem 2.4 implies that $\mathfrak{J}' < 0$ therefore the total number of infected subunits strictly decreases locally with time, or in other words, the epidemic is set to disappear.
- Better, (2.19) means that \mathfrak{J} almost surely converges exponentially to 0 or the epidemic disappears exponentially.
- These results mean that the contagion-free equilibrium point, if it exists, is locally asymptotically stable.

3. From the stochastic SIR to the impact on an insurance portfolio

Once the cyber contagion model is described, we are interested in the following questions concerning the distribution of the subunits' and firm's sizes, as well as the impact of the cyber contagion on the firm size growth, on a cyber insurance portfolio and more generally on the economy growth. Recall from (1.1) and (1.6), the revenue $Z_{i,t}$ of firm $i \in \{1, \dots, H\}$ at time $t \geq 0$, satisfies

$$Z_{i,t} = \sum_{j=1}^{K_i} z_{ij,t} = \sum_{j=1}^{K_i} (1 - \pi_{ij} \mathbf{1}_{\tau_{ij} \leq t < \tau_{ij} + \delta_{ij}}) \bar{z}_{ij,t},$$

where τ_{ij} is the first jump time of the point process N_{ij} and δ_{ij} is the random recovery time. The arrival of a cyber-attack can come either from outside or from a sister subunit. We thus have the following assumption.

Assumption 3.1. For $(i, j) \in \mathcal{I}$ and $t \geq 0$, we assume

$$N_{ij,t} := N_{ij,t}^0 + \mathbf{1}_{\left\{N_{ij,\tau_i^-}^0 = 0\right\}} \mathbf{1}_{\{t \geq \tau_i\}} U_{ij},$$

where

- $(N_{ij}^0)_{ij}$ is a sequence of independent Cox processes with common intensity Y defined in (2.5).
- τ_i is the stopping time defined as

$$\tau_i := \inf \left\{ t > 0 : \sum_{k=1}^{K_i} N_{ik,t}^0 \geq 1 \right\}. \quad (3.1)$$

- $(U_{ij})_{ij}$ is a sequence of iid Bernoulli random variables with probability a_{τ_i} .

In other words, for $(i, j) \in \mathcal{I}$ and $t \geq 0$, Theorem 3.1 states that:

- When the infection of subunit j of firm i comes from outside between t and $t+dt$, its probability is $Y_t dt$ where Y_t is the force of infection defined in (2.5). This implies that $\mathbb{E}[N_{ij,t+dt}^0 - N_{ij,t}^0 | \mathcal{F}_t^{\mathcal{W}}] = Y_t dt$ recalling that Y is $\mathbb{F}^{\mathcal{W}}$ -adapted (with $\mathbb{F}^{\mathcal{W}}$ given in (2.7)).
- When there exists at least one sister subunit of j infected from outside at time t i.e. $K_i > 1$ and $\sum_{k=1}^{K_i} N_{ik,t}^0 \geq 1$, and if the subunit j is not infected from outside at the time τ_i i.e. $N_{ij,\tau_i^-}^0 = 0$, then it may have an internal contagion U_{ij} with probability a_{τ_i} where a is the process defined in Assumption 2.1.

For each firm $1 \leq i \leq H$, if $K_i > 1$, the vector of point processes $(N_{ij})_{1 \leq j \leq K_i}$ is strongly correlated. We describe in the following proposition the marginal law of first jump of subunit j , namely τ_{ij} defined in (1.5).

Proposition 3.2. *For $(i, j) \in \mathcal{I}$, if $K_i \geq 2$, then the conditional marginal CDF function of τ_{ij} is, for $0 \leq u \leq t \leq T$*

$$F_{ij}^{|t}(u) := \mathbb{P}[\tau_{ij} \leq u | \mathcal{F}_t^{\mathcal{W}}] = 1 - e^{-K_i \Lambda_u} - (K_i - 1) e^{-\Lambda_u} \int_0^u Y_s e^{-(K_i-1)\Lambda_s} (1 - a_s) ds, \quad (3.2)$$

where $\Lambda_t := \int_0^t Y_s ds$.

Proof. Let $(i, j) \in \mathcal{I}$ and $0 \leq u \leq t \leq T$. If $K_i = 1$, there is no internal contagion. We directly have

$$\mathbb{P}[\tau_{ij} > u | \mathcal{F}_t^{\mathcal{W}}] = \mathbb{E} \left[\mathbf{1}_{N_{ij,u}^0 = 0} | \mathcal{F}_t^{\mathcal{W}} \right] = \mathbb{E} \left[\mathbb{E} \left[\mathbf{1}_{N_{ij,u}^0 = 0} | \mathcal{F}_u^{\mathcal{W}} \right] | \mathcal{F}_t^{\mathcal{W}} \right] = \mathbb{E} \left[e^{-\Lambda_u} | \mathcal{F}_t^{\mathcal{W}} \right] = e^{-\Lambda_u},$$

since Y is $\mathbb{F}^{\mathcal{W}}$ -adapted.

If $K_i \geq 2$, we decompose the set $\{\tau_{ij} > u\}$ in 2 disjoint sets $(\{N_{ij,u}^0 = 0\} \cap \{\tau_i > u\})$ and $(\{N_{ij,u}^0 = 0\} \cap \{\tau_i \leq u\} \cap \{U_{ij} = 0\})$. On the one hand

$$\mathbb{P}[\{N_{ij,u}^0 = 0\} \cap \{\tau_i > u\} | \mathcal{F}_t^{\mathcal{W}}] = \mathbb{P} \left[\bigcap_{k=1}^{K_i} \{N_{ik,u}^0 = 0\} | \mathcal{F}_t^{\mathcal{W}} \right] = e^{-K_i \Lambda_u},$$

where the last equality comes from the fact $(N_{ik}^0)_{ik}$ are iid conditionally to $\mathbb{F}^{\mathcal{W}}$. On the other hand,

$$\begin{aligned} \mathbb{P}[\{N_{ij,u}^0 = 0\} \cap \{\tau_i \leq u\} \cup \{U_{ij} = 0\} | \mathcal{F}_t^{\mathcal{W}}] &= \mathbb{P}[N_{ij,u}^0 = 0, \tau_i \leq u, U_{ij} = 0 | \mathcal{F}_t^{\mathcal{W}}] \\ &= \int_0^u \mathbb{P}[N_{ij,u}^0 = 0, \tau_i \in ds | \mathcal{F}_t^{\mathcal{W}}] (1 - a_s). \end{aligned}$$

$\mathbb{P}[N_{ij,u}^0 = 0, \tau_i \in ds | \mathcal{F}_t^{\mathcal{W}}] = \mathbb{P}[N_{ij,u}^0 = 0 | \mathcal{F}_t^{\mathcal{W}}] \mathbb{P}[\tau_i \in ds | N_{ij,u}^0 = 0, \mathcal{F}_t^{\mathcal{W}}]$, with $\mathbb{P}[N_{ij,u}^0 = 0 | \mathcal{F}_t^{\mathcal{W}}] = e^{-\Lambda_u}$, and

$$\begin{aligned} \mathbb{P}[\tau_i \in ds | N_{ij,u}^0 = 0, \mathcal{F}_t^{\mathcal{W}}] &= \frac{d}{ds} \mathbb{P}[\tau_i \leq s | N_{ij,u}^0 = 0, \mathcal{F}_t^{\mathcal{W}}] \\ &= -\frac{d}{ds} \mathbb{P} \left[\bigcap_{k=1, k \neq j}^{K_i} \{N_{ik,s}^0 = 0\} | \mathcal{F}_t^{\mathcal{W}} \right] \\ &= -\frac{d}{ds} e^{-(K_i-1)\Lambda_s} \\ &= (K_i - 1) Y_s e^{-(K_i-1)\Lambda_s}. \end{aligned}$$

Therefore,

$$\mathbb{P} [\{N_{ij,u}^0 = 0\} \cap \{\tau_i \leq u\} \cup \{U_{ij} = 0\} | \mathcal{F}_t^{\mathcal{W}}] = \int_0^u (K_i - 1) Y_s e^{-(K_i-1)\Lambda_s} (1 - a_s) e^{-\Lambda_u} ds.$$

Finally

$$\mathbb{P}[\tau_{ij} > u | \mathcal{F}_t^{\mathcal{W}}] = e^{-K_i \Lambda_u} + (K_i - 1) e^{-\Lambda_u} \int_0^u Y_s e^{-(K_i-1)\Lambda_s} (1 - a_s) ds,$$

and the conclusion follows. \square

Remark 3.3. Let $t \geq 0$. From (3.2), we can make the following remarks:

1. The right term does not depend on the subunit so that the marginal distributions of first jump of all subunits of the same firm are identical. We will denote $F_i^{|t}$ the $\mathcal{F}_t^{\mathcal{W}}$ -cumulative distribution function, instead of $F_{ij}^{|t}$.
2. The form of $F_i^{|t}$ implies that the $\mathcal{F}_t^{\mathcal{W}}$ -conditional probability that a subunit becomes infected increases with the probability of internal contagion.
3. For a fixed firm i at a fixed date t and for a fixed trajectory of \mathcal{W} , if the function $K_i \mapsto (K_i-1)\Lambda_s - 1$ is negative for all $0 \leq s \leq u$, then the function $K_i \mapsto F_i^{|t}(u)$ is non-decreasing. In fact, by differentiating the function $K_i \mapsto F_i^{|t}(u)$, we get

$$\begin{aligned} \frac{dF_i^{|t}(u)}{dK_i} &= K_i e^{-K_i \Lambda_u} - e^{-\Lambda_t} \int_0^u Y_s e^{-(K_i-1)\Lambda_s} (1 - a_s) ds + (K_i - 1) e^{-\Lambda_u} \int_0^u \Lambda_s Y_s e^{-(K_i-1)\Lambda_s} (1 - a_s) ds, \\ &= K_i e^{-K_i \Lambda_u} + e^{-\Lambda_u} \int_0^u [(K_i - 1)\Lambda_s - 1] Y_s e^{-(K_i-1)\Lambda_s} (1 - a_s) ds. \end{aligned}$$

This means that the $\mathcal{F}_t^{\mathcal{W}}$ -probability that a subunit becomes infected increases with the number of subunits. This is obvious in particular when the process (Λ_u) is bounded by $\frac{1}{K-1}$.

4. For all firms with the same size (number of subunits), all their subunits have the same $\mathcal{F}_t^{\mathcal{W}}$ -conditional probability to be infected at a given time.
5. Let $1 \leq i \leq H$ and $0 \leq u \leq t$. Because

$$\mathbb{P} \left[\bigcap_{k=1}^{K_i} \{N_{ik,u} = 0\} | \mathcal{F}_t^{\mathcal{W}} \right] = \mathbb{P} \left[\bigcap_{k=1}^{K_i} \{N_{ik,u}^0 = 0\} | \mathcal{F}_t^{\mathcal{W}} \right] = e^{-K_i \Lambda_u},$$

the $\mathcal{F}_t^{\mathcal{W}}$ -conditional probability that at least one subunit of firm i gets infected before time u is $1 - e^{-K_i \Lambda_u}$ which increases with K_i . Therefore, the vulnerability of firms increases with their size.

The marginal $\mathcal{F}_t^{\mathcal{W}}$ -conditional CDF (F_i) are obviously $\mathcal{F}_t^{\mathcal{W}}$ -measurable because a and Y are. In order to fully determine the firm revenue (see (1.1)) and firm claims (see (1.9)) under cyber-attack, we need to characterize the random recovery time (δ_{ij}) introduced in Assumption 1.2. We deduce (δ_{ij}) from the recovery rate process γ_i in the SIR model (2.4) as follows.

Assumption 3.4. For $(i, j) \in \mathcal{I}$, we assume that

$$\delta_{ij} = \frac{1}{\gamma_{i, \tau_{ij}}}. \quad (3.3)$$

This is motivated by the fact that when the recovery times of infected individuals are modeled as independent exponentially distributed random variables, the recovery rate is equal to the inverse of the expected recovery time (see Doenges et al. (2024)).

Moreover, we define the filtration $\mathbb{G} = (\mathcal{G}_t)_{t \geq 0}$ by

$$\mathcal{G}_t = \sigma \left(\mathcal{F}_t^B \cup \mathcal{F}_t^{\mathcal{W}} \cup \sigma \{ \pi_{ij,s}, N_{ij,s} : s \in [0, t] \text{ and } (i, j) \in \mathcal{I} \} \right), \quad (3.4)$$

where \mathcal{F}_t^B and $\mathcal{F}_t^{\mathcal{W}}$ are defined in (1.8) and in (2.7) respectively.

Remark 3.5. It is straightforward that the subunit revenue $(z_{ij})_{(i,j) \in \mathcal{I}}$, the total revenue of the portfolio \mathbf{O} , and the firm's claims $(c_{i,t})_{1 \leq i \leq H}$, defined respectively in (1.6), (1.7), and (1.9) are \mathbb{G} -adapted.

With the knowledge of $(\tau_{ij})_{ij}$ and $(\delta_{ij})_{ij}$, it is now possible to compute the costs of cyber-events at the firm level $(\mathbf{c}_i)_i$ from (1.9) and at the portfolio level AEP from (1.14). But let us note that other insurance portfolio measures can be studied, and in particular, the impact of reaction and remediation measures as in Hillairet and Lopez (2021).

From (1.9), we can identify 4 sources of randomness in the cost functions \mathbf{c} , \mathbf{C} , or AEP. The first one is the Brownian motion B governing the economic risk and represented by \mathbb{F}^B . The second one is the random coefficients of SIR represented by $\mathbb{F}^{\mathcal{W}}$, the third one is the random arrivals (τ_{ij}) of cyber-attacks, and the last one is their random severity π . In fact, all these quantities have a "systemic part" which is $\mathbb{F}^{\mathcal{W}}$ -adapted coming from the cyber-attack and an "idiosyncratic/economic part" which are (N_{ij}) , (π_{ij}) , (B_{ij}) . We can assume that the insurer mutualizes well the idiosyncratic/economic risks, as $(B_{ij})_{(i,j) \in \mathcal{I}}$ are independent between firms. Therefore we may focus on the systemic cyber risk component and consider $\mathbb{F}^{\mathcal{W}}$ as the only source of randomness by taking the expectation conditional to the systemic risk. This leads to the notion of conditional AEP *_T , without the idiosyncratic risk:

$$\text{AEP}^*_T(x) := 1 - \mathbb{E}_P \left[F_{\mathbf{C}_T^*}(x) \right], \quad (3.5)$$

where \mathbf{C}_T^* is the total expected loss conditionally to the random SIR factors up to t , $\mathcal{F}_t^{\mathcal{W}}$

$$\mathbf{C}_T^* := \sum_{i=1}^H \left(\int_0^T \mathbb{E} [c_{i,t} | \mathcal{F}_t^{\mathcal{W}}] dt \right),$$

and $c_{i,t}$ is defined in (1.9). The following proposition gives an explicit expression of $\mathbb{E} [c_{i,t} | \mathcal{F}_t^{\mathcal{W}}]$.

Proposition 3.6. For $1 \leq i \leq H$ and $t, u \geq 0$,

$$\mathbb{E} [c_{i,t} | \mathcal{F}_t^{\mathcal{W}}] = \left(\pi_{\star} \sum_{j=1}^{K_i} z_{ij,0} e^{\mu_{ij} t} \right) \int_0^t \mathbf{1}_{\{\gamma_{i,u} < \frac{1}{t-u}\}} dF_i^{|t}(u), \quad (3.6)$$

where F_i is defined in (3.2).

Proof. Let $1 \leq i \leq H$ and $t, u \geq 0$. From the explicit expression of the claims at t given in (1.9), we have:

$$\mathbb{E} [c_{i,t} | \mathcal{F}_t^{\mathcal{W}}] = \mathbb{E} \left[\sum_{j=1}^{K_i} \bar{z}_{ij,t} \pi_{ij} \mathbf{1}_{\tau_{ij} \leq t < \tau_{ij} + \delta_{ij}} | \mathcal{F}_t^{\mathcal{W}} \right].$$

Given that (π_{ij}) are independent of $\mathcal{F}_t^{\mathcal{W}}$ with $\mathbb{E}[\pi_{ij}] = \pi_{\star}$ and that, from Assumptions 1.2 and 2.1, $\mathbb{E}[z_{ij,t} | \mathcal{F}_t^{\mathcal{W}}] = \mathbb{E}[z_{ij,t}] = z_{ij,0} e^{\mu_{ij} t}$, we have

$$\mathbb{E} [c_{i,t} | \mathcal{F}_t^{\mathcal{W}}] = \pi_{\star} \sum_{j=1}^{K_i} z_{ij,0} e^{\mu_{ij} t} \mathbb{E} \left[\mathbf{1}_{\tau_{ij} \leq t < \tau_{ij} + \frac{1}{\gamma_{i,\tau_{ij}}}} \middle| \mathcal{F}_t^{\mathcal{W}} \right],$$

recalling from (3.3) that $\delta_{ij} = \frac{1}{\gamma_{i,\tau_{ij}}}$. For each $1 \leq j \leq K_i$,

$$\begin{aligned} \mathbb{E} \left[\mathbf{1}_{\left\{ \tau_{ij} \leq t < \tau_{ij} + \frac{1}{\gamma_{i,\tau_{ij}}} \right\}} \middle| \mathcal{F}_t^{\mathcal{W}} \right] &= \mathbb{E} \left[\mathbf{1}_{\left\{ t - \frac{1}{\gamma_{i,\tau_{ij}}} < \tau_{ij} \leq t \right\}} \middle| \mathcal{F}_t^{\mathcal{W}} \right] \\ &= \int_0^{+\infty} \mathbf{1}_{\left\{ t - \frac{1}{\gamma_{i,u}} < u \leq t \right\}} d\mathbb{P}(\tau_{ij} \leq u | \mathcal{F}_t^{\mathcal{W}}) \\ &= \int_0^t \mathbf{1}_{\{\gamma_{i,u} < \frac{1}{t-u}\}} d\mathbb{P}(\tau_{ij} \leq u | \mathcal{F}_t^{\mathcal{W}}). \end{aligned}$$

We conclude using $\mathbb{P}(\tau_{ij} \leq u | \mathcal{F}_t^{\mathcal{W}}) = F_i^{|t}(u)$ for $0 \leq u \leq t$ as given in Theorem 3.2. \square

After further straightforward calculations, we obtain

$$\mathfrak{C}_T^{\star} = \sum_{(i,j) \in \mathcal{I}} \frac{\pi_{\star} z_{ij,0}}{\mu_{ij}} \int_0^T \left(e^{\mu_{ij} \min\left(T, u + \frac{1}{\gamma_{i,u}}\right)} - e^{\mu_{ij} u} \right) dF_i^{|u}(u). \quad (3.7)$$

Computing \mathfrak{C}_T^{\star} is faster than \mathfrak{C}_T . Indeed, instead of simulating $|\mathcal{J}|$ random arrival times and integrating $|\mathcal{J}|$ geometric Brownian motion paths, we only need to evaluate $|\mathcal{J}|$ deterministic integrals. This reduction becomes particularly advantageous when the portfolio is large (i.e., when $|\mathcal{J}|$ or H is big). In our simulations, the size of the portfolio being reasonable, the distribution of C_T remains computationally tractable to compute the exact AEP. In Figure 14, we compare these exact AEP curves to those obtained for C_T^{\star} .

4. Numerical analysis and discussion

This section describes the data for parameters calibration and estimation, outlines the calibration methods and comments on the estimated parameters, and finally presents the simulation methodology and discusses the results.

4.1. The dataset

4.1.1. Firm’s data

The dataset Pappers (2025) provides information of $H = 2,929$ firms located in the Ile-de-France region, in particular the sector of activity (using the NAF classification as in Insee (2025)) and the annual revenue (in €million) from 2010 to 2022 (that is for $T^f = 13$ years). Table 1 summarizes firms’ characteristics – including the count, mean, and standard deviation of revenue– by sector.

Sector	Number of firms	Average revenue	Std of revenue
Manufacturing	339	7.13	12.18
Technology	87	5.85	10.09
Retail/Wholesale	788	9.91	18.11
Healthcare / Education / Government	65	2.03	3.54
Consulting / Legal	383	5.01	9.59
Construction	559	5.53	9.94
Banking/Finance	64	2.52	6.12
Miscellaneous**	644	3.73	—
Total	2929	2.87	13.04

Table 1: Firms characteristics. (**) Includes Agriculture, Mining, Transport, and Real Estate.

4.1.2. Cyber contagion data

Each quarter, the *GuidePoint Security’s Research and Intelligence Team* publishes a Ransomware and Cyber Threat Insights (see GuidePoint Security (2025) for the year 2024). This report summarizes cyber crime incidents, mainly ransomware attacks, that occurred during the year. Data collected are obtained from publicly available resources, including the sites and blogs of threat groups themselves. Figure 1b and Figure 3 summarize, respectively, the most impactful ransomware groups and the most impacted industries in 2024. For this numerical analysis, we calibrate the cyber-episode on the **LockBit** ransomware which, according to GuidePoint Security (2025), entered 2024 as the long-standing dominant ransomware group with the highest tempo by victim, but the group faced substantial disruption in the wake of February’s international operation Cronos (see Europol (2024)). The calibration and validation are done on the time interval from May 1, 2024 to July 31, 2024, that is $T = 100$ days.

The database gives the total infected per industry in 2024 for all the ransomware groups, the total infected per group day for each group. However, the data do not specify the number of infected firms by size. We address this by proposing a proxy in Section 4.2.2, based on the estimated firm size distribution.

Industry	Victims	Rate
Manufacturing	610	20.68%
Technology	390	13.22%
Retail/Wholesale	335	11.36%
Healthcare	325	11.02%
Consulting	275	9.32%
Construction	235	7.97%
Education	205	6.95%
Legal	200	6.78%
Government	190	6.44%
Banking/Finance	185	6.27%

Table 2: Most impacted industries in 2024

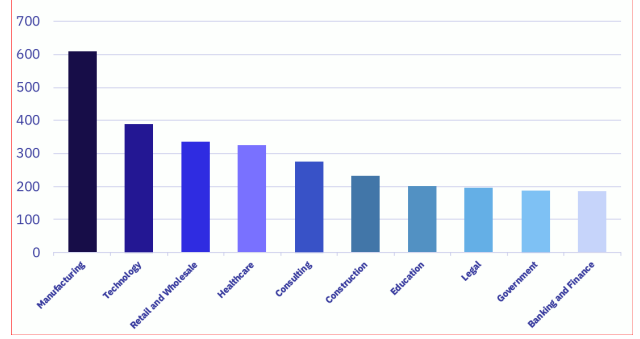


Figure 3: Industries impacted (x-axis: sector, y-axis: victims)

4.2. Calibration procedure

4.2.1. Calibration of the firms parameters

Recall that there are $H = 2,929$ firms in the portfolio. For each firm of the portfolio, we have annual revenue data $Z_{i,t}$ between year 1 (corresponding to 2010) and year $T^f = 13$ (corresponding to 2023). However, since we do not have the number of subsidiaries and their revenue, we construct the following proxy for both variables.

The empirical average of revenue in the database is written as

$$\bar{Z}_t = \frac{1}{H} \sum_{i=1}^H Z_{i,t}. \quad (4.1)$$

We assume that company $i \in \{1, \dots, H\}$ has a single subsidiary if its initial revenue $Z_{i,1}$ is below the initial sample average \bar{Z}_1 ; otherwise, it is assumed to have multiple subsidiaries. Formally,

$$K_i = \left\lceil \frac{Z_{i,1}}{\bar{Z}_1} \right\rceil \in \mathbb{N}^*, \quad (4.2)$$

where $\lceil x \rceil$ is the smallest integer greater than or equal to x . Then, assuming that all subsidiaries of a same firm have the same size, we have, for all $j \in \{1, \dots, K_i\}$,

$$z_{ij,t} = \frac{Z_{i,t}}{K_i}. \quad (4.3)$$

Then the estimation of the Black Scholes parameters (1.4), $(\sigma_{ij})_{(i,j) \in \mathcal{I}}$ and $(\mu_{ij})_{(i,j) \in \mathcal{I}}$, is given by

$$\sigma_{ij}^{\text{year}} = \sqrt{\frac{1}{T^f - 1} \sum_{t=1}^{T^f-1} (r_{ij,t} - r_{ij,*})^2}, \quad \text{and} \quad \mu_{ij}^{\text{year}} = r_{ij,*} + \frac{1}{2}(\sigma_{ij}^{\text{year}})^2,$$

where for each subsidiary, $r_{ij,t} := \log \frac{z_{ij,t+1}}{z_{ij,t}}$ is the revenue growth between two consecutive years and

$r_{ij,*} := \frac{1}{T^f - 1} \sum_{t=1}^{T^f-1} r_{ij,t}$ is the average revenue growth over the period T^f . Finally, since cyber-events are

tracked on a daily frequency, we convert the annual parameters to daily parameters by assuming 365 days:

$$\sigma_{ij} = \frac{\sigma_{ij}^{\text{year}}}{\sqrt{365}} \quad \text{and} \quad \mu_{ij}^{\text{year}} = \frac{\mu_{ij}^{\text{year}}}{365}.$$

We use the firms' revenue dataset described in Table 1 to determine the firms/subunit characteristics.

Table 3 below indicates the number of firms per size (i.e. the number of subunits) and per sector. The maximum firm size is $K = 12$. Figure 4a and Figure 4b show that the firm size is distributed

Sector	Firm size											
	1	2	3	4	5	6	7	8	9	10	11	12
Manufacturing	249	51	20	7	2	2	1	1	3	1	2	0
Technology	67	5	5	4	2	0	3	0	1	0	0	0
Retail/Wholesale	619	80	42	18	11	7	4	1	1	1	2	2
Healthcare/Education/Government	47	12	1	1	0	1	0	2	1	0	0	0
Consulting / Legal	317	31	22	6	1	2	1	0	1	2	0	0
Construction	433	62	30	11	7	4	3	5	2	1	0	1
Banking/Finance	57	2	0	2	1	1	0	0	1	0	0	0
Miscellaneous**	474	69	18	12	14	3	1	4	1	2	0	1
Total	2263	312	138	61	38	20	13	13	11	7	4	4

Table 3: Number of firms per size and per sector

according to Zipf law (see (1.3)); ; the fitted parameters are $\alpha = 1.759$ and $q = 0.784$. A small number of very large firms account for a large share of total mass, therefore aggregate quantities – such as AEP – are therefore sensitive to extreme firms.

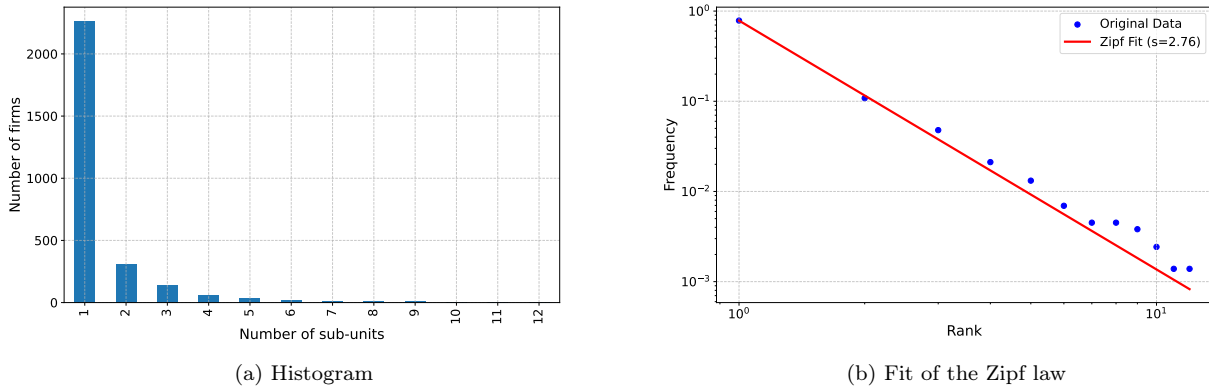


Figure 4: Firm size

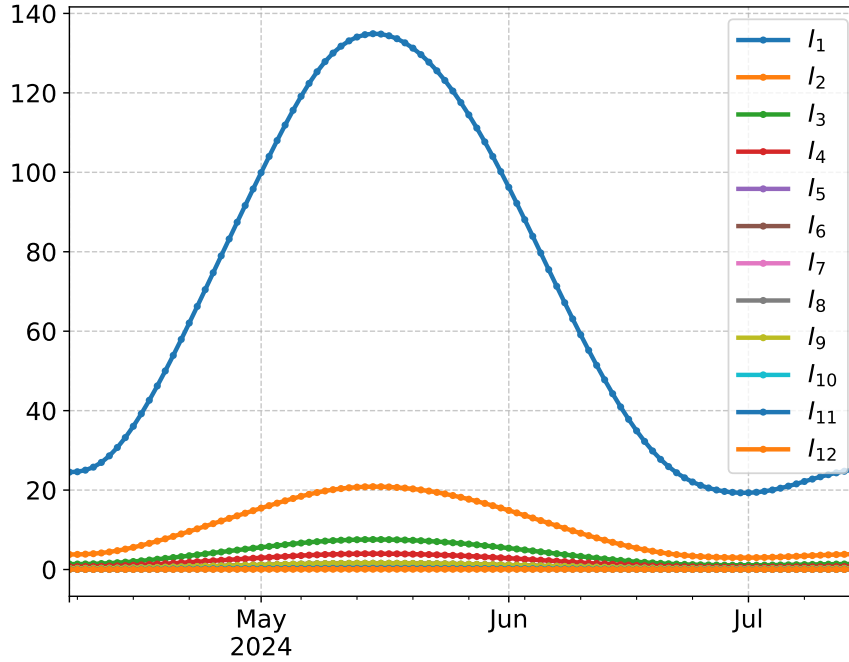
In Table 4, we summarize the average drift, the volatility, and the initial revenue, for each size.

K_i	1	2	3	4	5	6	7	8	9	10	11	12
z_{ij}^0 (in €million)	4.70	5.99	6.99	6.69	7.30	8.98	7.49	5.40	6.70	6.61	10.03	9.82
$\sigma_{ij} \times 10^3$	12.69	12.30	10.91	9.70	16.16	8.16	19.03	26.31	8.64	12.71	4.92	4.79
$\mu_{ij} \times 10^3$	0.19	0.37	0.28	0.26	0.56	0.24	1.12	1.45	0.36	0.28	0.33	0.27

Table 4: subunits' characteristics

4.2.2. Calibration of the SIR parameters

To build a proxy for the number of infected firms per size, we first divide the number of attacks per sector by the total number of attacks to get the attack rate per sector in 2024 (see Table 2). By multiplying the latter by the total number of LockBit infections, we obtain the average number of attacks per sector. Then, based on the distribution of subsidiaries across sectors in Table 3, we derive an estimate of the number of infected firms of varying sizes (see Figure 5).


Figure 5: Number of daily new firms infected per size each day in May - June - July 2024 (I_k)

To calibrate the SIR parameters, we follow the Optimization based on Forward Model Simulation approach proposed by Balan (2023), which is detailed below. It requires the numbers of susceptibles and recovered individuals in the beginning of the episode, and –most importantly– the daily counts of new infections throughout the epidemic.

From Section 4.2.1, the maximum firm size is $K := \max_{i \in \{1, \dots, H\}} K_i = 12$. The cyber episode runs from 1 May to 31 July 2024; we denote the daily observation dates by $\{t_0, t_1, \dots, t_T\}$. For calibration,

we have from the dataset the daily detected infections, $(i_{k,t_u})_{1 \leq k \leq K, 0 \leq u \leq T}$. We reasonably assume that the initial removed are zero i.e. $(r_{k,t_0} = 0)_{1 \leq k \leq K}$. As we do not have the initial number of susceptible population previously noted $(s_{k,t_0})_{1 \leq k \leq K}$, we consider them as model parameters.

Assuming the firm size distribution follows a Zipf law with parameters $\mathbf{a} = 1.759$ and $q = 0.784$ (see Equation (1.3)) for firm size in the insurance portfolio and the entire database, it is sufficient to consider the total number of firms h_\star as a model parameter since for all $k = 1 \dots K$,

$$h_{k,t_0} = \left\lfloor h_\star \frac{\frac{1}{k^{\mathbf{a}}}}{\sum_{j=1}^K \frac{1}{j^{\mathbf{a}}}} \right\rfloor, \quad (4.4)$$

with $h_{k,t_0} = s_{k,t_0} + i_{k,t_0} + r_{k,t_0}$. Here, $\lfloor x \rfloor$ denotes the floor function, representing the greatest integer less than or equal to x .

For the SIR model, the main challenge consists in calibrating the coefficients $\varphi_0, \mu_\varphi, \kappa_\varphi$, and Σ_φ of each stochastic SIR parameter $\varphi \in \Psi$, recalling from (2.13) that,

$$\tilde{\varphi}_t = \varphi_0 e^{-\kappa_\varphi t} + \mu_\varphi (1 - e^{-\kappa_\varphi t}) + \Sigma_\varphi \int_0^t e^{-\kappa_\varphi(t-s)} \sqrt{\tilde{\varphi}_s} d\mathcal{W}_{\varphi,s}.$$

In words, $\tilde{\varphi}$ is a CIR process where the speed of mean reversion is κ_φ , μ_φ the long-term mean level, Σ_φ the volatility factor and, φ_0 is the initial condition. We have at this stage $4 \times (2K + K^2)$ CIR coefficients to calibrate, that is 672 because $K = 12$. This is large relatively to the limited data at hand. In order to simplify and speed up the calibration, we make the following additional assumptions.

1. As stated in Theorem 2.3, $(b_{j,k})$ is binomial with in-firm attack rate a also governed by a CIR process.
2. All stochastic SIR parameters, modeled as CIR processes, share the same mean reversion speed and volatility coefficient. However, they possess different long-term mean levels, each set equal to its respective initial value, i.e. for all $\varphi \in \Psi$, $(\kappa_\varphi = \kappa_a)$, $(\Sigma_\varphi = \Sigma_a)$, and $(\mu_\varphi = \varphi_0)$.
3. As state in Doenges et al. (2024), for each size, when the out-firm reproduction number (β_k/γ_k) is independent of the firm size and the infections are parallel, the recovery rate γ_k is proportional to the inverse of the expected recovery time $\sum_{j=1}^k \frac{1}{j}$. We write

$$\gamma_k = \frac{\gamma_1}{\sum_{j=1}^k \frac{1}{j}} \quad \text{and} \quad \beta_k = \frac{\beta_1}{\sum_{j=1}^k \frac{1}{j}}, \quad (4.5)$$

where the last equality assumes that the decay rate of immunity is independent of the firm size. Therefore, it is enough to determine γ_1 and β_1 .

We therefore need to calibrate six coefficients: $\kappa_a, \Sigma_a, a_{t_0}, \gamma_{1,t_0}, \beta_{1,t_0}$, and h_\star , that are denoted as

$$\Theta := \{\kappa_a, \Sigma_a, a_{t_0}, \gamma_{1,t_0}, \beta_{1,t_0}, h_\star\}. \quad (4.6)$$

The calibration procedure for Θ is as follows. A set $\Theta \in (\mathbb{R}_+)^6$ of CIR coefficients be given, we simulate $M \in \mathbb{N}^*$ trajectories of the SIR parameters over the discrete time grid $\{t_0, t_1, \dots, t_T\}$ using the exact

simulation method for CIR processes described in Alfonsi (2015). For each parameter $\varphi \in \Psi$, we obtain the realizations $(\varphi_{t_u}^m)_{1 \leq m \leq M, 0 \leq u \leq T}$. Subsequently, for each trajectory $m \in \llbracket 1, M \rrbracket$, we evolve the SIR model using the following Euler scheme to generate $(S_k^m, I_k^m, R_k^m)_{1 \leq k \leq K}$. For $0 \leq u \leq T - 1$ and $1 \leq k \leq K$, the dynamics are given by:

$$\begin{cases} S_{k,t_{u+1}}^m - S_{k,t_u}^m = -kY_{t_u}^m S_{k,t_u}^m + Y_{t_u}^m \sum_{j=k+1}^K j S_{j,t_u}^m \cdot b_{jj-k,t_u}^m, \\ I_{k,t_{u+1}}^m - I_{k,t_u}^m = -\gamma_{k,t}^m I_{k,t_u}^m + Y_{t_u}^m \sum_{j=k}^K j S_{j,t_u}^m \cdot b_{jk,t_u}^m, \\ R_{k,t_{u+1}}^m - R_{k,t_u}^m = \gamma_{k,t_u}^m I_{k,t_u}^m, \end{cases} \quad \text{where } Y_{t_u}^m = \frac{1}{N_0} \sum_{k=1}^K \beta_{k,t_u}^m \cdot k I_{k,t_u}^m, \quad (4.7)$$

with initial conditions $I_{k,t_0}^m = I_{k,t_0}$, $R_{k,t_0}^m = 0$, and $S_{k,t_0}^m = S_{k,t_0}$. The optimal coefficient Θ_* minimizes the mean square error J_2 , between the historical number of infected (I_{k,t_u}) plotted on Figure 5 and the simulated trajectory (I_{k,t_u}^m), defined as

$$J_2(\Theta) := \frac{1}{M} \sum_{m=1}^M J_2^m(\Theta), \quad \text{with} \quad J_2^m(\Theta) := \sum_{k=1}^K \sum_{u=0}^T |I_{k,t_u} - I_{k,t_u}^m|^2. \quad (4.8)$$

The procedure is summarized in Algorithm 1. Table 5 gives the 6 calibrated parameters. We observe that (1) the volatility of the stochastic SIR parameters is low, and (2) the initial in-firm infection rate, $\frac{1}{1+e^{-a_{t_0}}} = 0.586$ is relatively high.

Initial recovery rate	γ_{1,t_0}	0.6782
Initial "out-firm" infection rate	β_{1,t_0}	0.5471
Initial in-firm attack rate	a_{t_0}	0.3466
Volatility	Σ_φ	0.0151
Mean reversion speed	μ_φ	0.4474
Total population of firms	h_*	14,210

Table 5: The SIR model parameters

The total number of firms h_* is used to calculate the initial population in each group, that we give in Table 6.

	H_1	H_2	H_3	H_4	H_5	H_6	H_7	H_8	H_9	H_{10}	H_{11}	H_{12}
Size	11144	1646	538	244	132	80	52	36	26	20	15	12

Table 6: The initial population per group

4.3. Estimation procedure of revenues and claims, simulations, and discussion

From the calibrated model coefficients Θ_* , we simulate M trajectories of the stochastic SIR parameters $(\varphi^m)_{\varphi \in \Psi, 1 \leq m \leq M}$ ($M = 10,000$ in this numerical analysis). For each trajectory m of parameters, we simulate the cyber-contagion using the Euler scheme for the SIR described in (4.7). We obtain, for each scenario $1 \leq m \leq M$, the force of epidemics $(Y_{t_u}^m)$.

Algorithm 1 SIR Calibration

- 1: **procedure** SIR CALIBRATION($K, T, (I_{k,t_u}), \mathbf{a}, q, M$)
 - 2: **Input:** Maximum firm size K , horizon of the cyber-episode T , number of infected $(i_{k,t_u})_{1 \leq k \leq K, 0 \leq u \leq T}$, Zipf law parameters \mathbf{a}, q .
 - 3: **for all** $\Theta = \{\kappa_a, \Sigma_a, a_{t_0}, \gamma_{1,t_0}, \beta_{1,t_0}, h_\star\}$ **do**
 - 4: Calculate the number of firms per size (h_{k,t_0}) using (4.4), then the initial number of susceptible using $(s_{k,t_0} = h_{k,t_0} - i_{k,t_0})$
 - 5: Convert numbers of susceptible into susceptible rates $S_{k,t_0} = \frac{s_{k,t_0}}{h_{k,t_0}}$, and numbers of infected into infection rates $I_{k,t_u} = \frac{i_{k,t_u}}{h_{k,t_0}}$.
 - 6: Calculate the average size $N_0 = \sum_{l=1}^K k(S_{k,t_0} + I_{k,t_0})$.
 - 7: Simulate M trajectories $(\varphi_t^m)_{1 \leq m \leq M, 0 \leq t \leq T}$ for each $\varphi \in \Psi$ on $\{0, 1, \dots, T\}$.
 - 8: **for all** $(\varphi_{t_u}^m)_{\varphi \in \Psi, 0 \leq u \leq T}$ **do**
 - 9: Simulate a forward SIR model with parameters $(\varphi_{t_u}^m)$ and initial condition $I_{k,t_0}^m = I_{k,t_0}$, $R_{k,t_0}^m = 0$, $I_{k,t_0}^m = I_{k,t_0}$, as well as N_0 , and obtain daily time series $(S_k^m, I_k^m, R_k^m)_{1 \leq k \leq K}$.
 - 10: Compute the objective function $J_2^m(\Theta)$.
 - 11: **end for**
 - 12: Compute the objective function $J_2(\Theta)$.
 - 13: **end for**
 - 14: Determine the minimum and the minimizer Θ of J_2 .
 - 15: **Output:** the parameters $\Theta = (\kappa_a, \Sigma_a, a_{t_0}, \gamma_{1,t_0}, \beta_{1,t_0}, h_\star)$.
 - 16: **end procedure**
-

Simulation of the arrival of cyber-attack on each firm (and on each subunit). We fix the scenario $1 \leq m \leq M$. For each firm $1 \leq i \leq H$, we simulate $(\tau_{ij}^m)_{1 \leq j \leq K_i, 0 \leq u \leq T}$ as follows:

1. Primary (or out-firm) infections: for each subunit $1 \leq j \leq K_i$, we simulate the first jump of the Cox process $(N_{ij,t_u}^{0,m,sim})_{0 \leq u \leq T}$ with intensity $(Y_{t_u}^m)_{0 \leq u \leq T}$.
2. Determine the time of the very first cyber-attack in the firm i , τ_i^m using (3.1) with the convention $\tau_i^m = T + 1$ if $\sum_{j=1}^{K_i} N_{ij,T}^{0,m,sim} = 0$. This means that firm i is not suffering from a primary infection. If $K_i = 1$, then $\tau_{i,j}^m = \tau_i^m$.
3. If $K_i \geq 2$ and $\tau_i^m \leq T$ (that is firm i has many subunits and at least one is externally infected), then secondary (or in-firm) infections can occur: for each $1 \leq j \leq K_i$, if $N_{ij,\tau_i^m}^{0,m,sim} = 0$ (that is subunit j is not yet infected), simulate a random variable U_{ij}^m with success parameter $a_{\tau_i^m}^m$
 - if $U_{ij}^m = 1$, set $\tau_{i,j}^m = \tau_i^m$,
 - else, set $\tau_{i,j}^m = T + 1$ (subunit j is not suffering from either a primary infection or a secondary infection).
4. If $K_i \geq 2$ and $\tau_i^m = T + 1$, $\tau_{i,j}^m = +\infty$ for all $1 \leq j \leq K_i$.

Simulation of the costs. We simulate also M realizations of $(\pi_{ij}^m)_{1 \leq m \leq M}$ of the random variables π_{ij} for $(i, j) \in \mathcal{I}$, to compute the Monte Carlo approximation of the total instantaneous expected revenue at each date of the cyber episode using the last equality of (1.7): for each $0 \leq u \leq T$

$$\mathbb{E}[\mathbf{O}_{t_u}] \approx \sum_{i=1}^H \sum_{j=1}^{K_i} z_{ij,0} e^{\mu_{ij} u} \left(1 - \frac{1}{M} \sum_{m=1}^M \pi_{ij}^m \mathbf{1}_{\tau_{i,j}^m \leq t_u < \tau_{i,j}^m + \frac{1}{\gamma_{i,\tau_{i,j}^m}^m}} \right). \quad (4.9)$$

For all $1 \leq i \leq H$, the daily claims of firm i for each scenario m and at each date t_u , $\mathbf{C}_{i,[t_u, t_{u+1}]}^m$, is given, using (1.11), by the trapezoidal method between $t_u \vee \tau_{i,j}^m$ and $t_{u+1} \wedge \left(\tau_{i,j}^m + \frac{1}{\gamma_{i,\tau_{i,j}^m}^m} \right)$. We then approach the cumulative distribution function (cdf) of the portfolio at each date t_u , with $u \in \{0, 1, \dots, T\}$

$$\mathbf{F}_{[t_u, t_{u+1}]}(x) = \mathbb{P} \left(\sum_{i=1}^H C_{i,[t_u, t_{u+1}]} \leq x \right), \quad x \geq 0,$$

by the empirical cdf

$$\widehat{\mathbf{F}}_{[t_u, t_{u+1}]}^M(x) := \frac{1}{M} \sum_{m=1}^M \mathbf{1}_{\left\{ \sum_{i=1}^H C_{i,[t_u, t_{u+1}]}^m \leq x \right\}}, \quad (4.10)$$

where $\mathbf{1}_{(X > x)}$ is the indicator function that equals 1 if $X > x$, and 0 otherwise. Algorithm 2 details the procedure for the compute of $\mathbf{F}_{[u, u+1]}^M(x)$. Finally, we compute the Aggregate Exceedance Probability

Algorithm 2 Calculate CDF \mathbf{F}

procedure $\mathbf{F}(x, T, M, \alpha^\pi, \beta^\pi, \Theta, (S_{k,t_0}, I_{k,t_0}, R_{k,t_0}))$.

Input: quantile x , horizon T , number of simulations M , the set of coefficients of the SIR parameters Θ , the initial values of the SIR $(S_{k,t_0}, I_{k,t_0}, R_{k,t_0})_{1 \leq k \leq K}$, parameters of severity (α^π, β^π) , and the parameters of firms $(z_{ij,t_0}, \mu_{ij}, \sigma_{ij})_{(i,j) \in \mathcal{I}}$.

for all Scenario $1 \leq m \leq M$ **do**

 From Θ , simulate a trajectory of the set of SIR parameters Ψ . ▷ Line 1

 Simulate a SIR model with parameter Ψ and initial condition $(S_{k,t_0}, I_{k,t_0}, R_{k,t_0})_{1 \leq k \leq K}$.

 Simulate the infection times.

 Simulate a trajectory of severity with (α^π, β^π) .

for all Date $1 \leq u \leq T$ **do**

 Calculate the set of infected firms at time u .

 Calculate the total claims at t_u using $\sum_{i=1}^H C_{i,[t_u, t_{u+1}]}^m$. ▷ Line 6

end for

 Calculate \mathbf{F} at u from (4.10).

end for

Output: The cumulative distribution function of daily losses \mathbf{F} .

end procedure

(AEP) over $[0, T]$ defined in (1.13) by performing Monte Carlo simulations described in Algorithm 3 with $M_P = 10,000$.

Algorithm 3 Calculate AEP

procedure AEP(x, v, M_P and parameters of \mathbf{F} in Algorithm 2)

Input: AEP threshold x , number of simulations of AEP M_P , intensity of Poisson random variable v .

Simulate M_P times $P \sim \text{Poisson}(v)$ and get $(P_m)_{m \in [1, M_P]}$.

for all P_m **do**

 Simulate P_m the loss \mathfrak{C}_T by repeatedly executing *Line 1* to *Line 6* of Algorithm 2 on the interval $[t_0, t_T]$ instead of $[t_u, t_{u+1}]$ and get $(\mathfrak{C}_T^{l,m})_{1 \leq l \leq P_m}$.

end for

$$\text{Calculate } \text{AEP}_T(x) = \frac{1}{M_P} \sum_{m=1}^{M_P} \mathbf{1} \left\{ \sum_{l=1}^{P_m} \mathfrak{C}_T^{l,m} > x \right\}.$$

Output: The aggregate exceedance probability AEP_T at T .

end procedure

4.3.1. Results of the contagion model

To compare the realized dynamics of the cyber-contagion (see Figure 5) with the simulated ones, we focus on the daily number of infected subunits, the peak defined in (2.15), and the date at which it occurs. Figure 6 illustrates the Lockbit trajectory (black) alongside the 99% confidence interval (blue) for the simulated dynamics over $T = 100$ days, based on $M = 10,000$ trajectories. Initial inspection of the results indicates that the model aligns closely with the observed epidemic trajectory: both the observed and mean simulated trajectories begin from the same initial condition (32 infected firms equivalent to 49 infected subunits) and reach their peak – defined as the maximum of the averaged trajectory – on day 38. While the peak date is identical, our model overestimates the observed peak by 17.15%. As in Hillairet and Lopez (2021), the peak (and the date it is reached) can be used to model the limited capacity of the insurance company to respond to an incident. If the number of policyholders needing help is too large, the insurer’s assistance teams can become overloaded. Figure 7b displays the distribution of peak dates across all simulated trajectories. The predicted peak is in close alignment with the realized peak: it predicts 317 infected subunits (to be compared to 273 observed), representing a 16.12% overestimation. Notably, while the observed peak occurs on day 38, the model accurately predicts the same peak date, with a maximum absolute deviation of 12 days across all simulations. In fact, it is preferable to slightly overestimate both the peak and underestimate the date at which it is reached, thereby yielding conservative risk measures.

We now examine the dynamics of contagion by firms size. Figure 8 represents the evolution of susceptible (Figure 8a), infected (Figure 8b), and recovered (Figure 8c) firms by size. The three dynamics follow a similar pattern – characterized by rapid growth toward a peak followed by a steady decline. However, different sizes reach their respective peaks at different dates. The peak dates by firm size are summarized in Table 7.

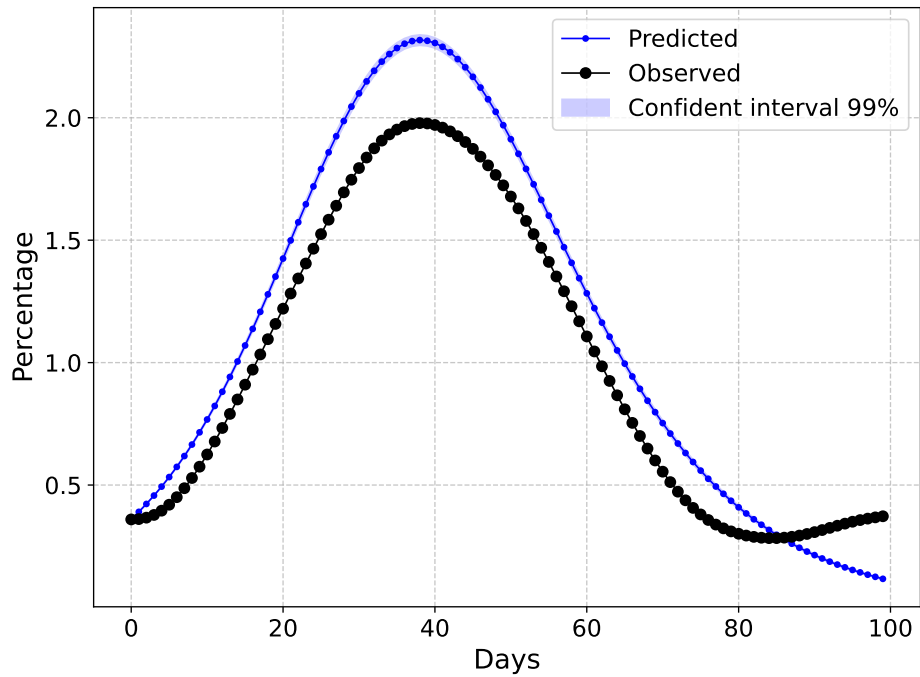
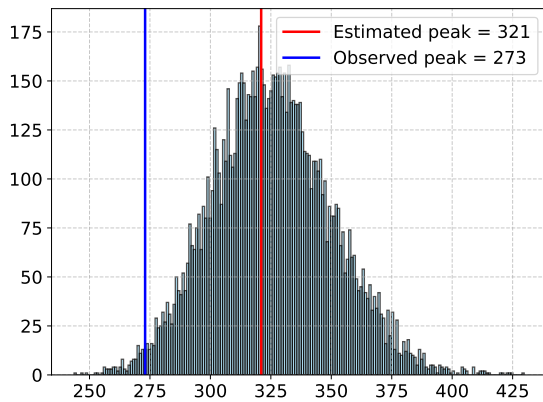
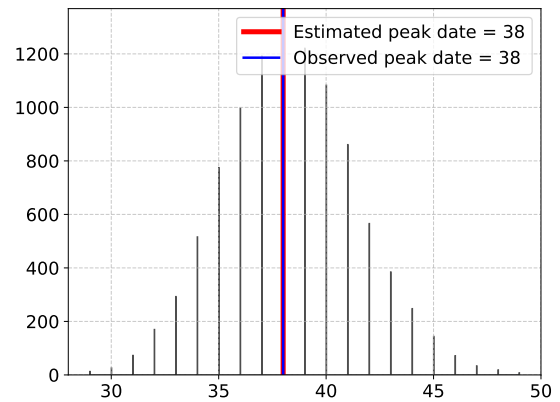


Figure 6: The dynamics of the total number of infected subunits, as percentage of the total population h_*



(a) The value of the peak



(b) The date at which the peak is reached

Figure 7: Histograms

For each group, the epidemic dynamics exhibit a consistent temporal ordering. For firms of size 1, the peak is closest or equal to the peak of epidemics (i.e. the maximum of the total number of infected subunits for all the size). This is consistent with the fact that this group represents 78% of companies. For firms of size 2 to 8, the peak in the number of infected and recovered individuals occur at the same time. This is consistent because the recovery rate is particularly high ($\gamma_{1,t_0} = 0.678$ in Table 5)

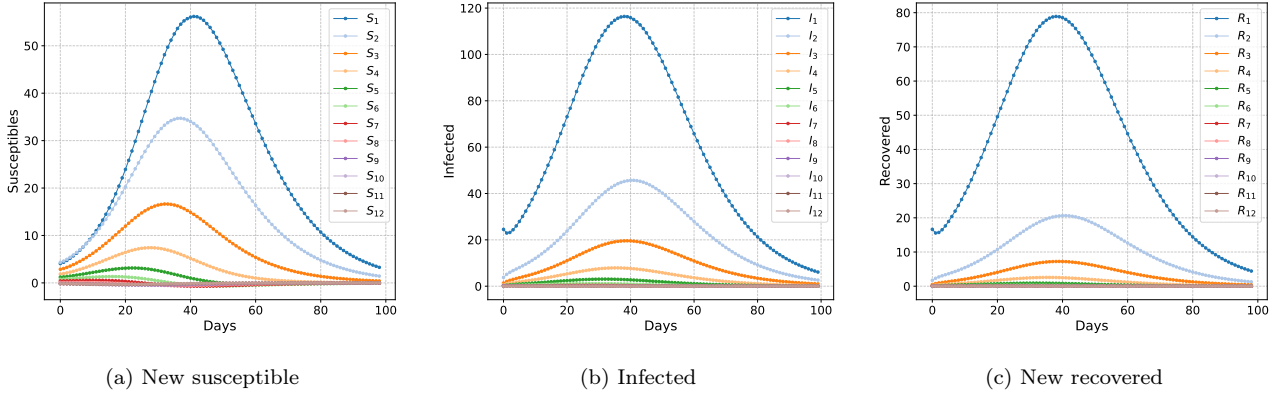


Figure 8: Evolution of the population in each group as percentage of the initial population in the group (see Table 6)

$k =$	1	2	3	4	5	6	7	8-12
New susceptibles height date	41	37	33	28	22	16	11	0
Infected height date	38	40	39	35	32	28	26	0
Recovered height date	38	40	39	35	32	28	26	0

Table 7: The date of the peak’s height per size

which, according to Doenges et al. (2024), is proportional to the inverse of the expected recovery time. The peak in the susceptible population for each size occurs before the peak of the total infected population. The peak decreases as the size increases, indicating a collapse of the epidemics in the larger organizational units first. This is partly due to the structure of the model, in which large firms feed into small ones. Moreover, since firm’s size follows Zipf’s law, there are much less firms with big size than small size. In our example, there are exactly 109 firms from size 8 to 12 which is 0.77% of the population (see Table 6). Thus, large companies very quickly reach their peak (right from the start of the epidemic here as shown in the last column of Table 7). Additional analyzes of the contagion model – especially regarding parameter sensitivity – can be conducted, drawing inspiration from Doenges et al. (2024).

We now turn to the probabilities of internal and external contagion. Figure 9 shows, for each day of the epidemic, the probability that the infection of a subunit originates outside the firm. This probability is low, though not zero and mirrors the epidemic dynamics, with a peak around day 38. By contrast, the probability that the infection of a subunit comes from another subunit within the same firm that we denoted $\frac{1}{1+e^{-a}}$, is high ($> 58\%$ calculated using the parameters Table 5) and, as assumed, independent of the progression of the epidemic. In summary, the likelihood that a firm becomes infected is small; however, once infection occurs, there is a significant chance that multiple subunits will be affected.

4.3.2. Impact of the contagion on a given firm

This section aims to examine the broader impact of contagion on the economy (see (1.7)) or its representative firms (i.e. the arithmetic mean of firms per size $1 \leq k \leq K$, $\bar{Z}_t^{(k)} := \frac{\sum_{i=1}^H \mathbf{1}_{\{K_i=k\}} Z_{i,t}}{\sum_{i=1}^H \mathbf{1}_{\{K_i=k\}}}$). It

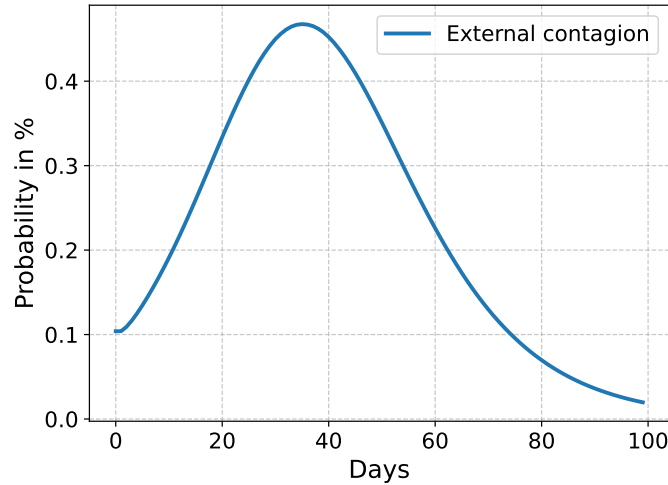


Figure 9: Probability of external infection

is important to recall that contagion effects stem from the organizational structure of the firms within the portfolio – specifically, the distribution of firm sizes and the presence of subsidiary networks. While current data constraints preclude the estimation of firm-specific or sectoral cost differences, the model is designed with the flexibility to incorporate these factors should the data become available.

As introduced in Theorem 1.2, when a subunit undergoes a cyber-attack, its revenue negatively jumps by $\pi \sim \mathcal{B}(\alpha^\pi, \beta^\pi)$. For the following simulations, we assume $\alpha^\pi = 50$ and $\beta^\pi = 10$ giving a mean loss of 0.833 with a standard deviation of 0.048. We start by calculating K_i for each firm i and $z_{0,ij}$, μ_{ij} , σ_{ij} for each subunit j of firm i . Then we run $M = 10,000$ scenarios corresponding to the simulation of the first arrival times of the cyber-event τ_{ij} and of the severity π_{ij} .

We plot on Figure 10 the probability density function of the infection time for different firm size i.e. $(\tau_k)_{1 \leq k \leq 12}$. Since we focus on the first 100 days of the epidemic, the event $\{\tau_k \geq 100\}$ – whose probability is reported in Table 8– corresponds to ‘no infection’ within the first 100 days..

$k =$	1	2	3	4	5	6	7	8	9	10	11	12
$\mathbb{P}[\tau_k > 100]$	0.794	0.623	0.500	0.394	0.310	0.249	0.194	0.150	0.129	0.095	0.069	0.060

Table 8: Probability of no infection ($\tau_k > 100$)

From Table 8, we observe that the larger the firm, the lower the probability that it becomes infected. In Figure 10, the distribution mode – the point at which the probability density reaches its maximum – is reached well before (on day 24) the peak of the epidemic (which only occurs on day 38). This mode naturally decreases with the size of the company. This means that the larger the size, the greater the chance that the firm will be infected before the peak is reached. Therefore, our model reproduces the stylized fact of cyber-episodes mentioned in Baksy et al. (2025); Kamiya et al. (2021).

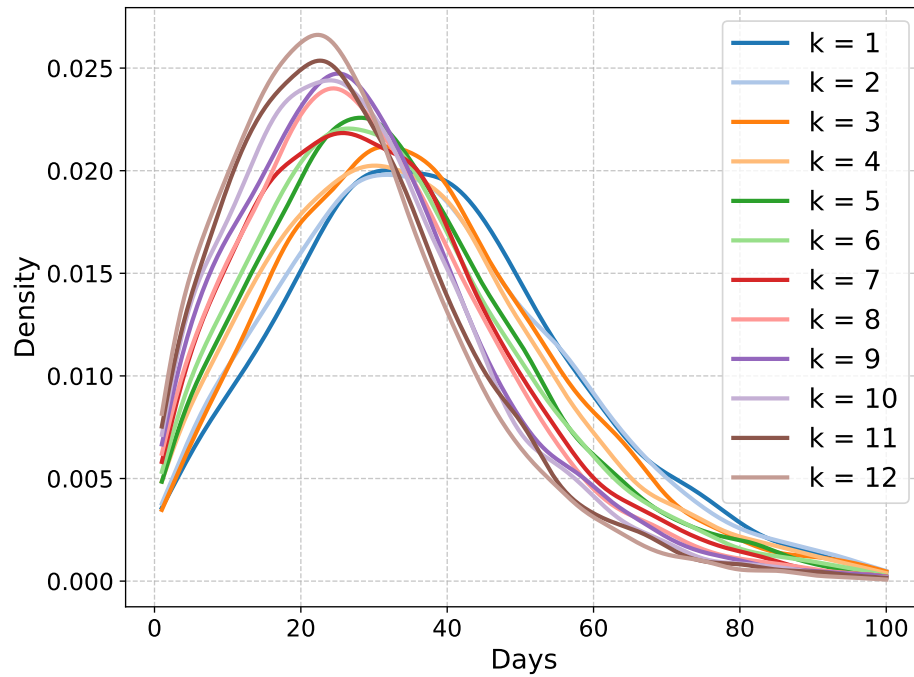


Figure 10: PDF of the infection time

For each group $k = 1, \dots, 12$, we plot on Figure 11a the average daily firm's claim as a percentage of the daily revenue, calculated across $M = 10,000$ simulations. As expected, for all sizes, the potential

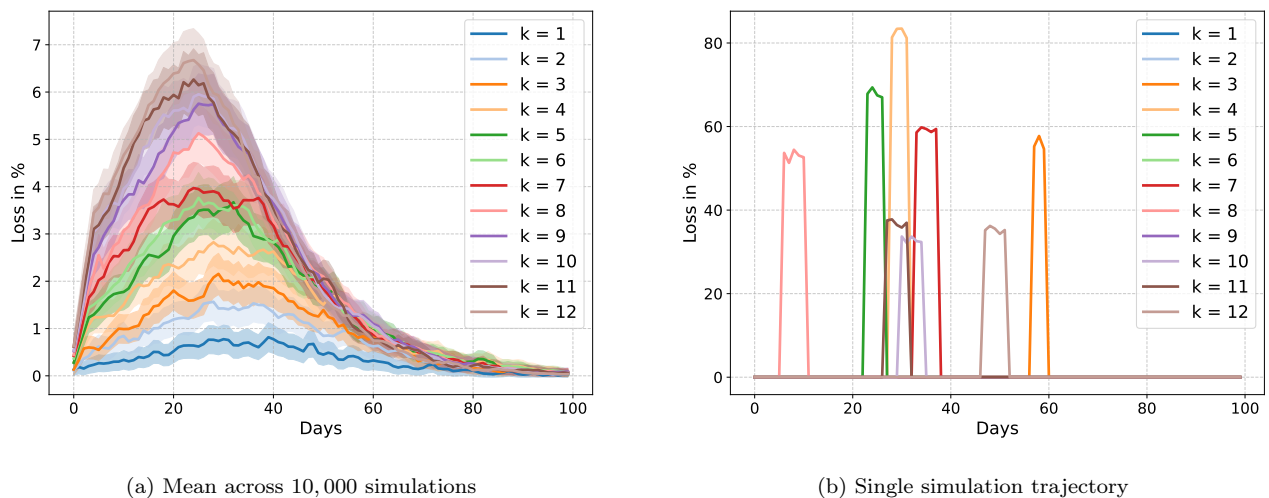


Figure 11: Daily revenue loss by firm size

loss of firm is naturally correlated with the date of initial infection. Furthermore, the losses increase with the number of subunits, clearly implying that size is an aggravating factor. This is due to internal

contamination between subsidiaries whose probability is 58.6%.

While an average daily loss peaking at 7% may appear low, this figure masks the underlying volatility. If we move beyond the mean of 10,000 simulations and consider a single contagion scenario, the picture changes significantly. As illustrated in Figure 11b, even with sporadic attacks, the claims relative to daily revenue can be substantial, occasionally reaching 75%. This extreme variance underscores the critical need for insurance. Furthermore, the duration of the infection increases with company size, as reflected by the recovery period $\delta_{ij} = \frac{1}{\gamma_i, \tau_{ij}}$ defined in (3.3).

4.3.3. Impact of the contagion on an insurance portfolio

We now proceed to the computation of the Aggregate Exceedance Probability (AEP) outlined in Algorithm 3. We begin by analyzing the PDF and the tails of the portfolio daily losses using their CDF computed in Algorithm 2. Given that small businesses typically hold fewer insurance policies, we focus on companies with a size greater than or equal to 2 ($K_i \geq 2$). This subset comprises 621 firms whose total revenue on the first day of the cyber-episode is €39.13 million.

Probability density function (PDF) of portfolio daily losses. We simulate $M = 10,000$ scenarios of the epidemic which gives M trajectories of the daily total losses $\sum_{i=1}^{621} C_{i,[t_u, t_{u+1}]}$ defined in (1.11). We analyze results on 5 different dates: $t_u = 7$ (7 days after the beginning of the epidemic), $t_u = 24$ (14 days before the peak), $t_u = 38$ (the peak date), $t_u = 52$ (14 days after the peak), and $t_u = 93$ (7 days before the end of the epidemic).

Figure 12a and Table 9 provides the PDF of portfolio daily losses. We observe that the closer we are

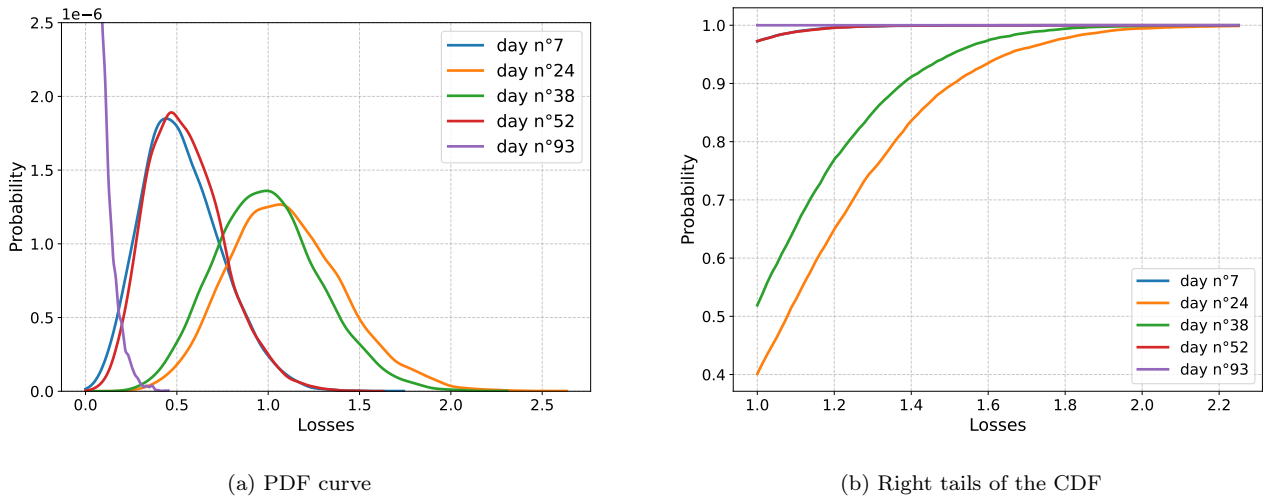


Figure 12: Daily financial impact in €million

to the peak of the cyber-event, the wider and flatter the total claims distribution is. This increased dispersion is most pronounced around day 24, coinciding with the period of highest infection probability – the mode of the infection-time distribution – as shown in Figure 10. The distribution’s support widens near the peak of the cyber-contagion, and both its mean and mode are higher around that point than

on other days. It can also be noted that the mode and the mean of the distribution at $t_u = 7$ are larger than at $t_u = 93$, reflecting a rapid decline. To summarize, the cyber-event induces a deformation in the distribution of total losses: as the contagion nears its peak (roughly between days 24 and 52), the PDF of daily losses becomes increasingly flattened, reflecting a broader dispersion around the mode.

Day	7	24	38	52	93
Lower bound	0	0	0	0	0
Upper bound	1.742	2.634	2.309	1.630	0.453
Mode	0.441	1.062	0.991	0.470	0.001
Mean	0.871	1.317	1.154	0.815	0.227

Table 9: Characteristics of the distribution’s support (in €million)

The losses on x-axis are in million euros and should be compared to the average daily revenue of a company in the portfolio, i.e. €39.13 million. In other words, we could expect a daily claim of up to 6.729% of €39.13 million. Let zoom on the right tail of the distribution.

Right tails of distribution of the portfolio daily losses. We consider claims from €1 million (2.56% of the average daily revenue of the portfolio) to €2.634 million (6.729%) using the empirical CDF given in (4.10). Figure 12b illustrates the right tails of the portfolio daily losses at 5 different dates. Consistent with the PDF deformation on Figure 12a, the right tail of distribution of daily losses thickens with the severity of the cyber-event. On day 24 when the mode of first arrival time is reached, the tail is the heaviest and the probability that the portfolio daily losses exceed €1 million reaches 60% whereas it remains negligible around the initial and terminal phases of the epidemic.

Similar as in Figure 12, Figure 13a and Figure 13b provides the PDF and the right tails of the total losses incurred by the sub-portfolio of 621 firms (with size K_i greater or equal 2) $\mathfrak{C}_T = \sum_{i=1}^{621} C_{i,[t_0,t_{100}]}$, over the 100-day duration of the cyber-episode. The PDF curve in Figure 13a suggests that the total claims after 100-day may range approximately up to €60.44 million, with a median greater than €51.47 million and a mode equals to €51.43 million. Moreover, the right tail in Figure 13b indicates that the total losses after 100 days exceeds €55 million with a probability around 6%. In practical terms, given a total daily revenue of €39.13 million, there is a risk that the total claims from a single 100-day cyber-episode will exceed 1.5 days of aggregate revenue for all firms in the sub-portfolio.

Aggregate Exceedance Probability (AEP) of the whole portfolio. Figure 14 displays the exact AEP curve (in blue), computed via \mathfrak{C}_T in (1.12), alongside the approximated AEP curve (in red), computed via \mathfrak{C}_T^* in (3.7). These results are obtained using Algorithm 3 with $M_P = 10,000$ and an average of $v = 0.105$ cyber-episodes per $T = 100$ days. This means that there is a 10% probability that a contagious cyber-episode occurs within 100 days (see Table 10).

The exact AEP curve on Figure 14a shows that, since the probability that no event occurs is about 90%, most of the mass of the distribution is zero. Moreover, even with an average of only 0.1 cyber-episode over 100 days, distribution support appears to extend to €180 million – roughly four days of revenue for the entire portfolio. We subsequently adopt a log-scale to better visualize this tail and

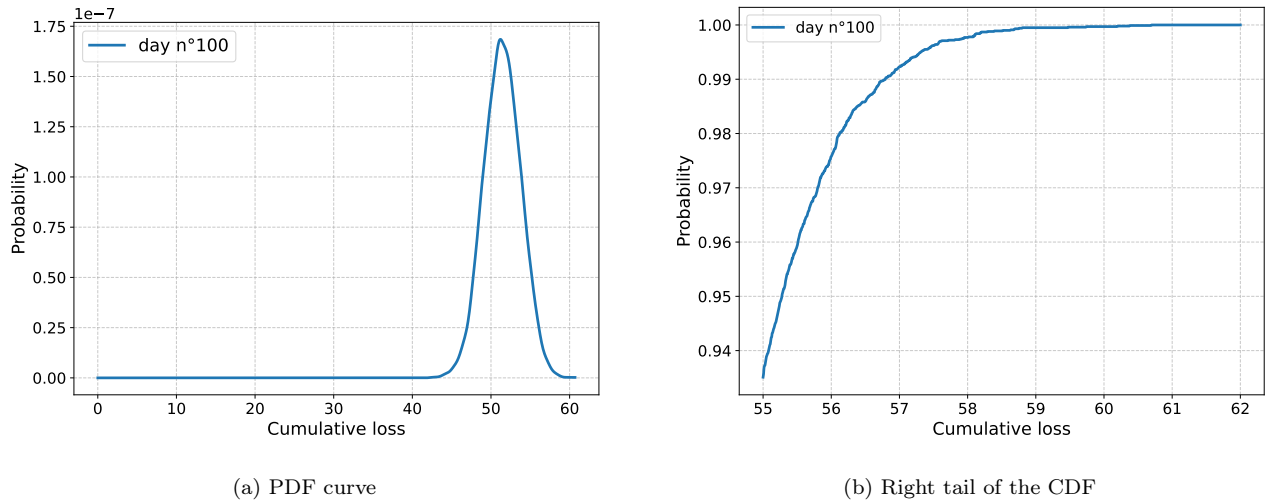


Figure 13: Financial impact after 100 days of the epidemic

	$P = 0$	$P = 1$	$P = 2$	$P \geq 3$
Probability (%)	90.0	9.45	0.496	0.054

Table 10: Poisson distribution with parameter $\nu = 0.105$.

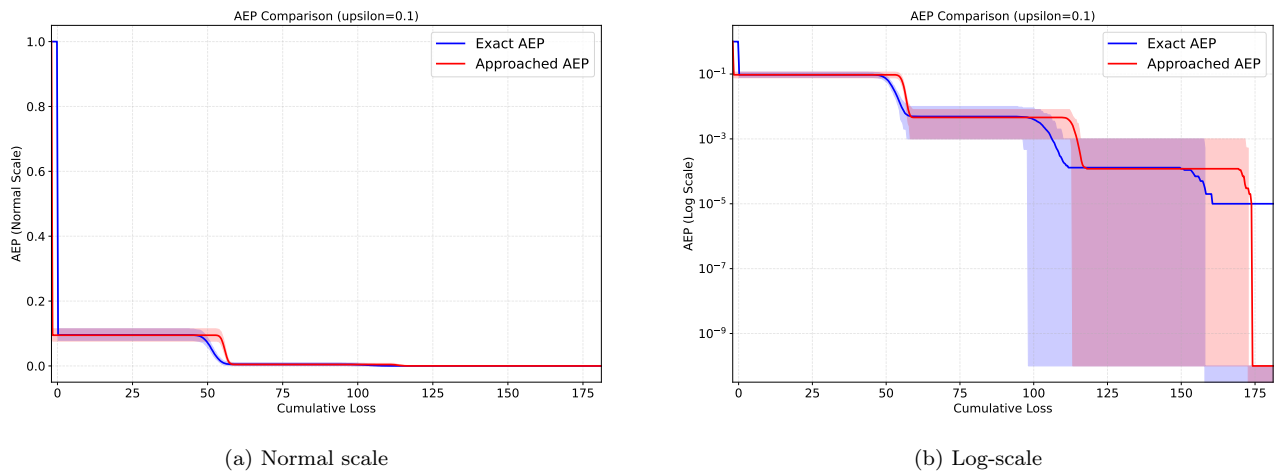


Figure 14: Exact (in blue) and approached AEP (in red) curves (the sum of losses are in € million)

to analyze the behavior conditional on the occurrence of cyber-episodes. The exact EAP curve on Figure 14b illustrates that, when an event occurs, total losses range from 0 to €180 million with a decreasing, sometimes very small but strictly positive probability. As expected from the definition of AEP, the curve is composed of successive segments: the part between 0 and €60 million corresponds to $F_{\mathbf{C}_{100}}$; the section between roughly €60 and €120 million reflects the 2-fold convolution of $F_{\mathbf{C}_{100}}$; and the tail between €120 and €180 million corresponds to the 3-fold convolution. Additionally, the

initial flat portion of the curve stems directly from the shape of the single-episode loss distribution: conditional on an event, the probability that total losses fall below €40 million is zero (see Figure 13a). Finally, the approached AEP (the red curve in Figure 14, computed from \mathfrak{C}_T^* defined in (3.7)) provides a good approximation of the exact AEP: it remains in the same range (up to €180 million) and exhibits the same jump structure. However, the jumps are noticeably steeper, and the approximation (that does not take into account the idiosyncratic risk) slightly underestimates the probability of the most extreme events. In our example, the portfolio is relatively small ($H = 621$ firms), so the AEP approximation is less relevant and the computational gain is negligible. For large-scale portfolios, by contrast, idiosyncratic risk mutualization operates more effectively and averaging out that risk becomes meaningful. The resulting computational efficiency is then significant enough that the slight underestimation of the AEP becomes an acceptable trade-off.

The analysis can be extended by calculating the AEP and PDF by activity's sector, by company size, and according to many other factors. We may also adopt different frequencies to examine how losses evolve on a weekly or monthly basis. Ultimately, the appropriate frequency and level of aggregation depend on the specific structure of the insurance portfolio.

Conclusion

This paper proposes a stochastic multigroup SIR model coupled with a granular model of firm growth, incorporating stylized facts from economics and cybersecurity to describe the propagation of cyber-episodes within a cyber-insurance portfolio. We provide quantitative analysis of the impact of such an event on firms' revenue dynamics and on an insurance portfolio. The model shows that the infection of a subunit most likely originates from another subunit within the same firm, not from outside. Moreover, larger firms experience more internal transmission, leading to greater losses and higher insurance claims. This extends the previous works of Hillairet and Lopez (2021); Hillairet et al. (2022) and provides a more comprehensive framework to assess the impact of a cyber-event on an economy or an insurance portfolio, under multiple scenario configurations.

References

- Alfonsi, A. (2015). Simulation of the CIR process. In *Affine Diffusions and Related Processes: Simulation, Theory and Applications*, pages 67–92. Springer.
- Allen, E. (2016). Environmental variability and mean-reverting processes. *Discrete Contin. Dyn. Syst. Ser. B*, 21(7):2073–2089.
- AXA Group (2025). Future risks report 2025. Accessed: 2026-02-10.
- Axtell, R. L. (2001). Zipf distribution of us firm sizes. *science*, 293(5536):1818–1820.
- Baksy, A., Caratelli, D., and Olson, L. M. (2025). Cyberattacks and firm size: The vulnerability of mid-size firms. Office of Financial Research, The OFR Blog.

- Balan, R. (2023). Lecture 9: Full calibration of SIR models. Lecture notes (Math 420), Department of Mathematics, University of Maryland. Version: February 23, 2023.
- Bessy-Roland, Y., Boumezoued, A., and Hillairet, C. (2021). Multivariate Hawkes process for cyber insurance. Annals of Actuarial Science, 15(1):14–39.
- Boumezoued, A., Cherkaoui, Y., and Hillairet, C. (2025). Cyber risk frequency modelling using Hawkes processes: Calibration on attack and vulnerability data. <https://hal.science/hal-05305048v1>.
- Bouzalmat, I., El Idrissi, M., Settati, A., and Lahrouz, A. (2023). Stochastic SIRS epidemic model with perturbation on immunity decay rate. Journal of Applied Mathematics and Computing, 69(6):4499–4524.
- Cox, J. C., Ingersoll, J. E., Ross, S. A., et al. (1985). A theory of the term structure of interest rates. Econometrica, 53(2):385–407.
- Doenges, P., Götz, T., Kruchinina, N., Krüger, T., Niedziewski, K., Priesemann, V., and Schäfer, M. (2024). SIR model for households. SIAM Journal on Applied Mathematics, 84(4):1460–1481.
- Edwards, B., Hofmeyr, S., and Forrest, S. (2016). Hype and heavy tails: A closer look at data breaches. Journal of Cybersecurity, 2(1):3–14.
- Eling, M. and Loperfido, N. (2017). Data breaches: Goodness of fit, pricing, and risk measurement. Insurance: Mathematics and Economics, 75:126–136.
- European Central Bank (2025). Cyber resilience stress testing: A macroprudential approach. Macroprudential Bulletin, Issue 22.
- Europol (2024). Law enforcement disrupt world’s biggest ransomware operation. Accessed: 2025-11-27.
- Farkas, S., Lopez, O., and Thomas, M. (2021). Cyber claim analysis using generalized Pareto regression trees with applications to insurance. Insurance: Mathematics and Economics, 98:92–105.
- Grossi, P., Kunreuther, H., and Patel, C. C. (2005). Catastrophe modeling: a new approach to managing risk, volume 25. Springer Science & Business Media.
- GuidePoint Security (2025). GRIT 2025 Ransomware & Cyber threat report. Technical report, GuidePoint Security. Accessed: 2025-08-15.
- Guo, H., Li, M. Y., and Shuai, Z. (2006). Global stability of the endemic equilibrium of multigroup SIR epidemic models. Canadian applied mathematics quarterly, 14(3):259–284.
- Herskovic, B., Kelly, B., Lustig, H., and Van Nieuwerburgh, S. (2020). Firm volatility in granular networks. Journal of Political Economy, 128(11):4097–4162.
- Hillairet, C. and Lopez, O. (2021). Propagation of cyber incidents in an insurance portfolio: counting processes combined with compartmental epidemiological models. Scandinavian Actuarial Journal, 2021(8):671–694.
- Hillairet, C., Lopez, O., d’Oultremont, L., and Spoorenberg, B. (2022). Cyber contagion: impact of the network structure on the losses of an insurance portfolio. Insurance: Mathematics and Economics.
- Homer, D. and Li, M. (2017). Notes on using property catastrophe model results. In Casualty Actuarial Society E-Forum, volume 2, pages 1–15.

- Insee (2025). French classification of activities. Accessed on 27 November 2025.
- Ji, C., Jiang, D., and Shi, N. (2011). Multigroup SIR epidemic model with stochastic perturbation. Physica A: Statistical Mechanics and its Applications, 390(10):1747–1762.
- Kamiya, S., Kang, J.-K., Kim, J., Milidonis, A., and Stulz, R. M. (2021). Risk management, firm reputation, and the impact of successful cyberattacks on target firms. Journal of Financial Economics, 139(3):719–749.
- Moran, J., Secchi, A., and Bouchaud, J.-P. (2024). Revisiting granular models of firm growth. Working paper.
- Pappers (2025). Pappers : Toute l’information gratuite sur les entreprises en France. Consulté le 26 novembre 2025.
- Peng, C., Xu, M., Xu, S., and Hu, T. (2017). Modeling and predicting extreme cyber attack rates via marked point processes. Journal of Applied Statistics, 44(14):2534–2563.
- Stanley, M. H., Amaral, L. A., Buldyrev, S. V., Havlin, S., Leschhorn, H., Maass, P., Salinger, M. A., and Stanley, H. E. (1996). Scaling behaviour in the growth of companies. Nature, 379(6568):804–806.
- Van den Driessche, P. and Watmough, J. (2002). Reproduction numbers and sub-threshold endemic equilibria for compartmental models of disease transmission. Mathematical biosciences, 180(1-2):29–48.
- Wyart, M. and Bouchaud, J.-P. (2003). Statistical models for company growth. Physica A: Statistical Mechanics and its Applications, 326(1-2):241–255.
- Zeller, G. and Scherer, M. (2022). A comprehensive model for cyber risk based on marked point processes and its application to insurance. European Actuarial Journal, 12(1):33–85.